

# **Astr 511: Galactic Astronomy**

Winter Quarter 2015, University of Washington, Željko Ivezić

## Lecture 7:

Stellar metallicity distribution in the Milky Way

# Outline

1. Introduction
2. SDSS stellar spectroscopic survey
3. Photometric Metallicity
4. Stellar Metallicity Distribution in the Milky Way
5.  $[\alpha/Fe]$  distribution for disk stars

## Reading:

- Reid & Hawley: ch. 7 and 8; Binney & Merrifield: ch. 10

## Introduction: metallicity

- Given the mass fraction of hydrogen,  $X$ , and the fraction of helium  $Y$ , the fraction of all the remaining chemical elements is  $Z = 1 - X - Y$ .
- For the Sun,  $X_{\odot} = 0.73$ ,  $Y_{\odot} = 0.25$  and  $Z_{\odot} = 0.02$ .
- Metallicity is defined, using *the numbers of atoms*, as  $[Fe/H] = \log_{10} (N_{Fe}/N_H)_* - \log_{10} (N_{Fe}/N_H)_{\odot}$ .
- The following proportionality is usually assumed, with  $C \sim 1$  (to within 10% or so),  
$$[M/H] \equiv \log_{10} \left( \frac{Z/X}{Z_*/X_*} \right) = C [Fe/H].$$
- Confusingly, both  $[M/H]$  and  $[Fe/H]$  are called “metallicity”.

## Introduction: $\alpha$ elements

- $\alpha$  elements are produced by the  $\alpha$  process, one of the two main nuclear fusion process responsible for the production of heavy elements from helium (the other one is the triple  $\alpha$  process). Their most abundant isotopes are integer multiples of four ( $\alpha$  particle is the helium nucleus) and have atomic number up to 22.
- $\alpha$  elements include O, Ne, Mg, Si, S, Ar, Ca, Ti.
- $\alpha$  elements are important for understanding the star formation history because Type II supernovae mainly synthesize oxygen and the  $\alpha$  elements, while Type Ia supernovae produce elements of the iron peak (V, Cr, Mn, Fe, Co and Ni).
- The progenitors of Type II supernovae are massive stars: short time scales, while Type Ia supernovae are due to white dwarfs: long time scales.

Figure 6: Type Ia SNe progenitor structure

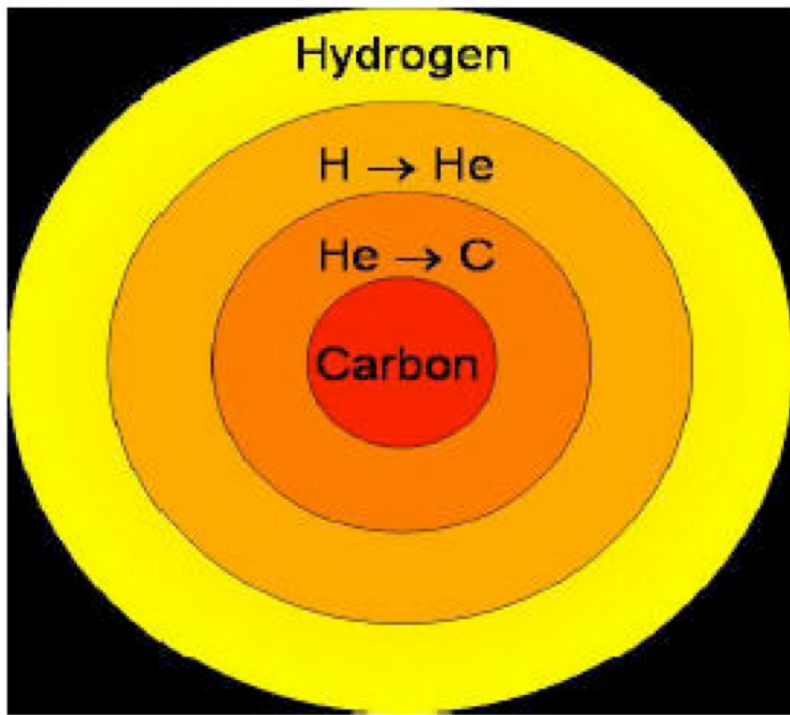
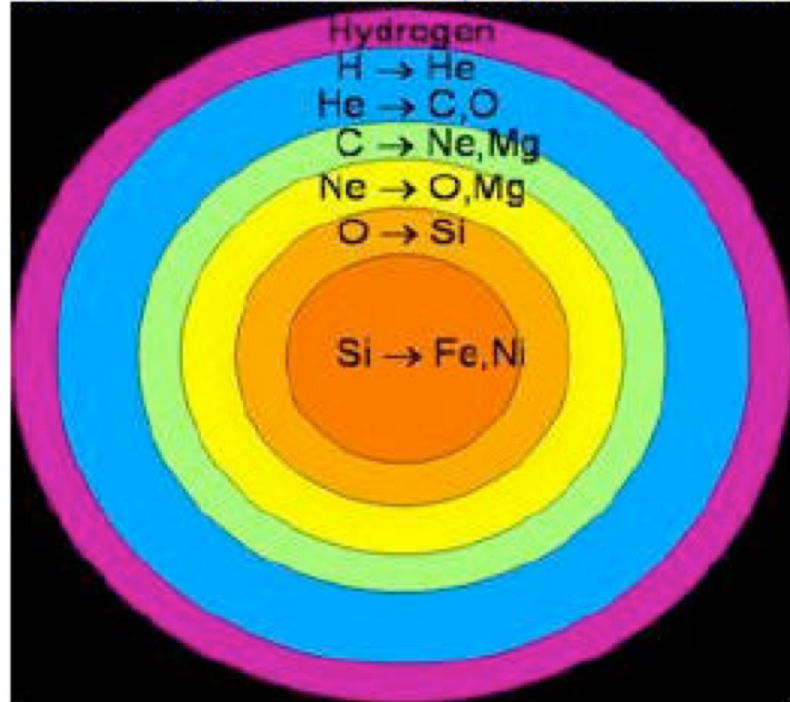
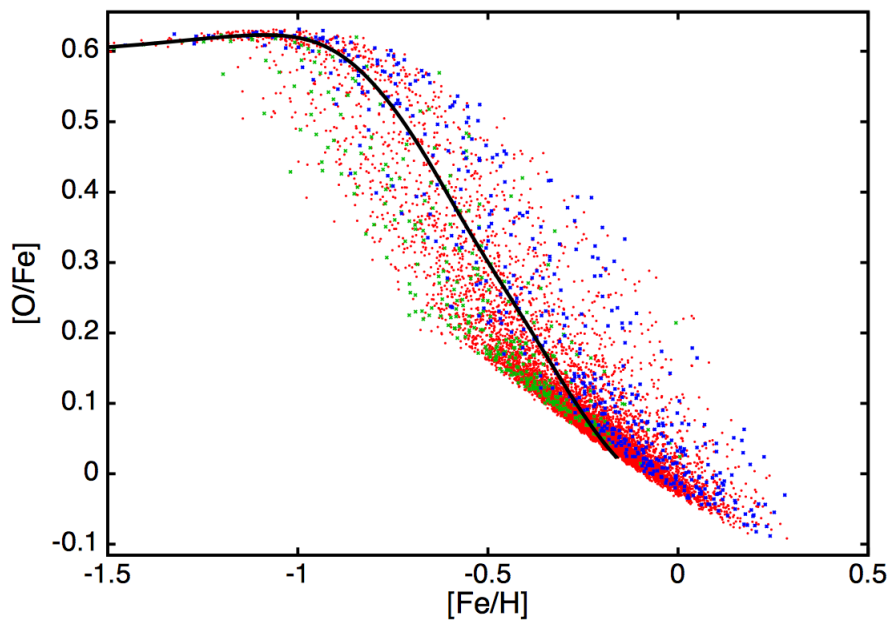


Figure 7: Type Ib, c & II SN progenitor structure



## Chemical yields of SNe

- Type II (core collapse) supernovae: short time scales and net increase of both  $[\alpha/Fe]$  and  $[Fe/H]$ .
- Type Ia supernovae are due to a white dwarfs in binary systems that accrete mass above the Chandrasekhar mass limit ( $1.4 M_{\odot}$ ) and explode in a runaway fusion reaction (standard candles,  $M_V = -19.3$ , important for cosmology!).
- Type Ia supernovae: long time scales (of the order 1 Gyr after Type II) and net increase of  $[Fe/H]$ , while  $[\alpha/Fe]$  is **decreasing**!



**Figure 9.** The predicted distribution of solar-neighbourhood stars in the ( $[Fe/H]$ ,  $[O/Fe]$ ) plane. The sample is obtained by using the selection function of the GCS survey as described in

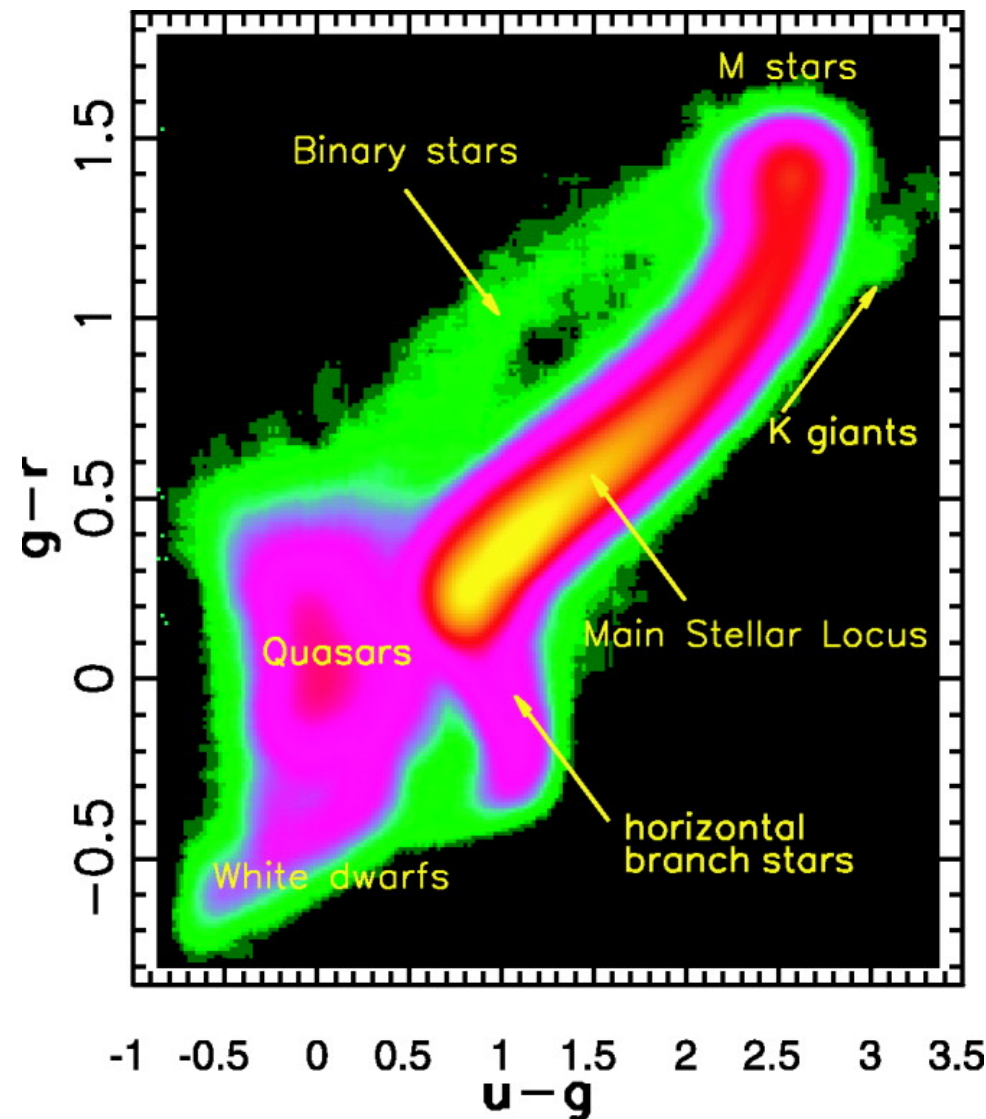
Model-based distribution from Schönrich & Binney (2009, MNRAS 396, 203). It shows the predicted distribution of stars from the solar neighbourhood (with a selection function from the Geneva-Copenhagen survey).

## Generic model prediction for the path through the $[\alpha/Fe]$ vs. $[Fe/H]$ diagram

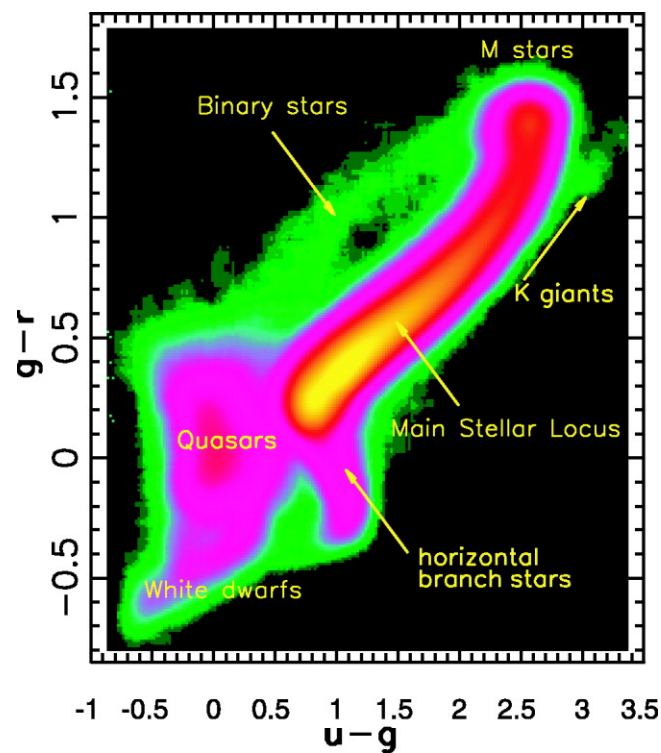
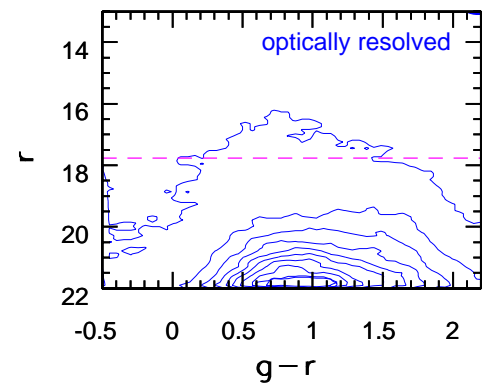
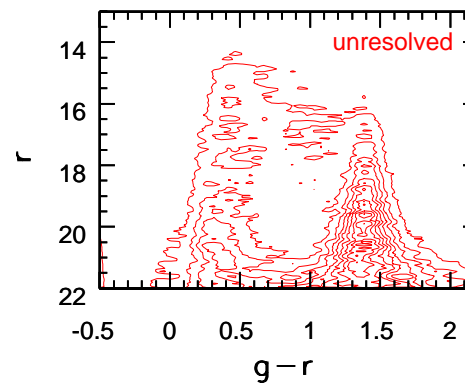
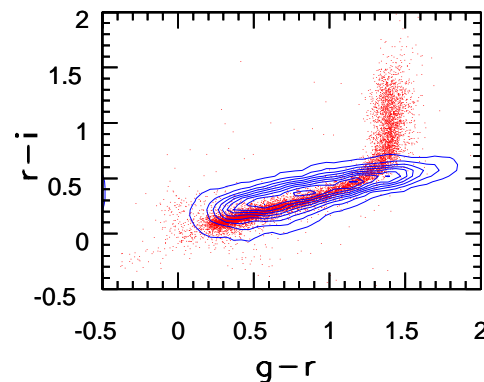
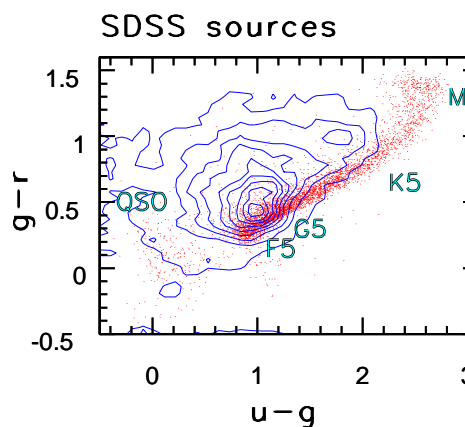
- A population of stars starts at high  $[O/Fe]$  and low  $[Fe/H]$ , upper left, and moves towards the lower right corner.
- *The curve is parametrized by time, increasing from the top left towards the lower right.*
- Quantitative details depend on star formation rate as a function of time, SN rates and their chemical yields, selection function, etc.
- Ongoing observational progress: is the observed bimodal structure a selection effect or not?

## Stars in SDSS

- Stars on the main stellar locus are dominated ( $\sim 98\%$ ) by main sequence stars (below  $r \sim 14$ )
- The position of main sequence stars on the locus is controlled by their spectral type/effective temperature/luminosity, and thus can be used to estimate distance: photometric parallax method for  $\sim 50$  million stars
- Accurate  $u - g$  color enables photometric metallicity estimates for 6 million SDSS F/G stars: needs calibration
- “Very interesting” stars are selected for SDSS spectroscopic follow-up



Wide wavelength coverage,  
and accurate and robust  
photometry



## Spectroscopic Targets:

- **Galaxies:** simple flux limit for “main” galaxies, flux-color cut for luminous red galaxies (cD)
- **Quasars:** flux-color cut, matches to FIRST survey
- **Non-tiled objects (color-selected):** calibration stars (16/640), interesting stars (hot white dwarfs, brown dwarfs (tiled), red dwarfs, C stars, CV, BHB, PN stars), sky

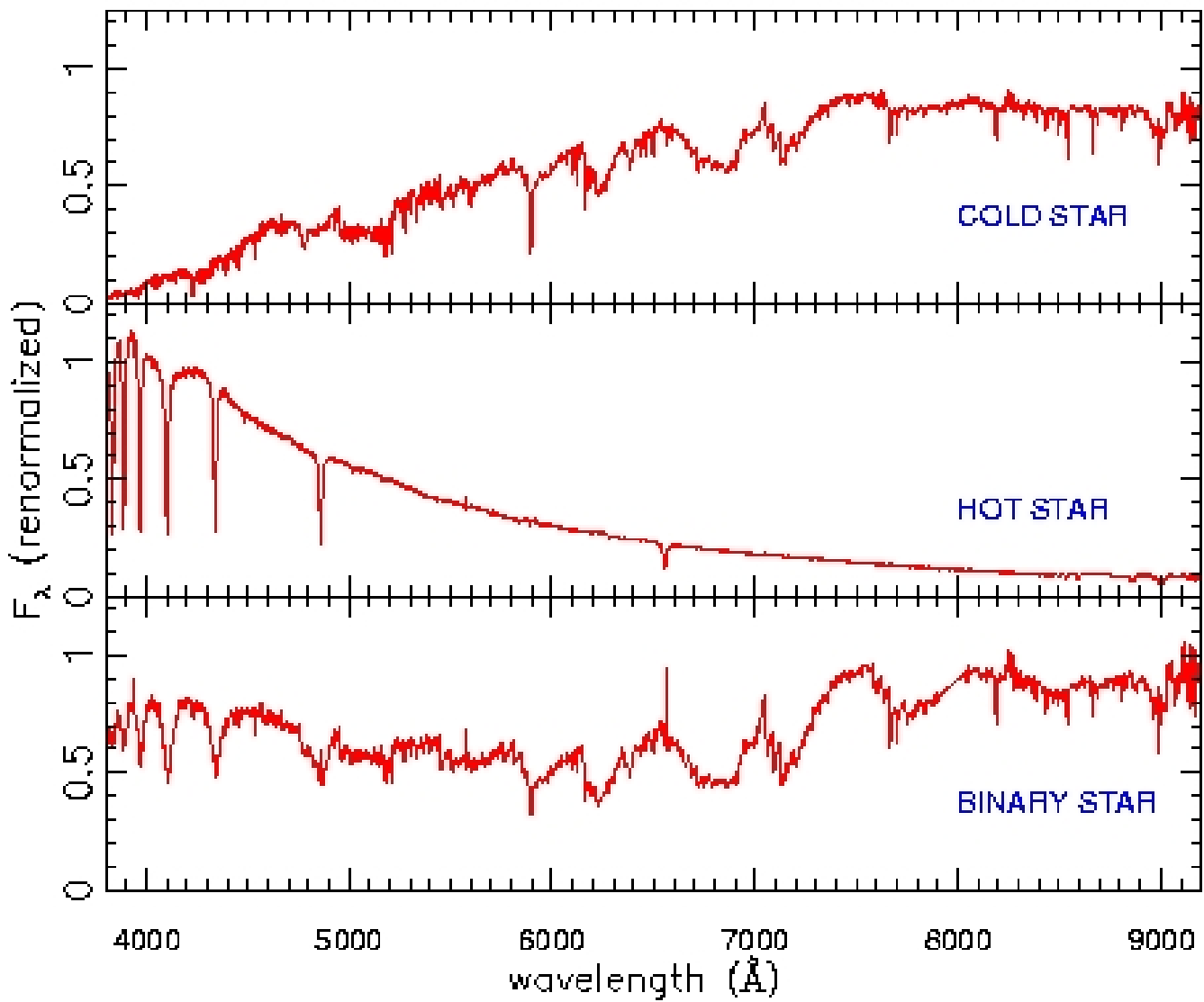
**SDSS Data Release 12:  
spectra for 2.4 million  
galaxies, 500,000 quasars,  
850,000 stars (and 200,000  
unknown!).**

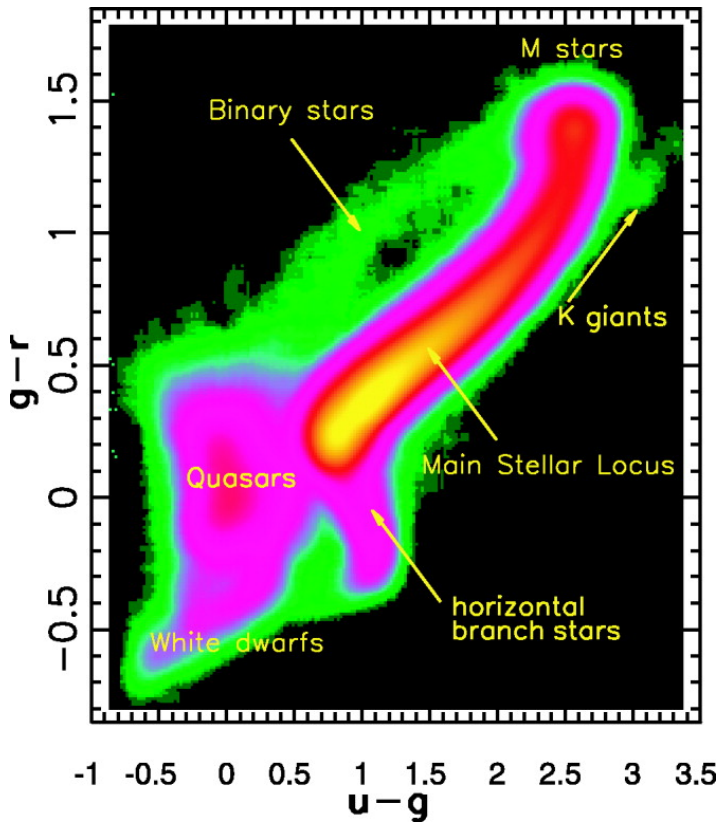
# Spectroscopic Data and Processing

- **Spectra:** Wavelength coverage: 3800–9200 Ang, Resolution: 1800, Signal-to-noise: >4 per pixel at  $g=20.2$ : *These spectra have much better quality than needed for a redshift survey of galaxies*; they are publicly available in a user-friendly format through an exquisite web interface at [www.sdss.org](http://www.sdss.org)
- **Automated Pipelines:**
  - *target*: target selection and tiling
  - *spectro2d*: Extraction of spectra, sky subtraction, wavelength and flux calibration, combination of multiple exposures: end result is a spectrum  $F_\lambda(\lambda)$
  - *spectro1d*: Uses  $F_\lambda(\lambda)$  for object classification, redshifts determination, measures line strengths and line indices.

# The Utility of SDSS Stellar Spectra

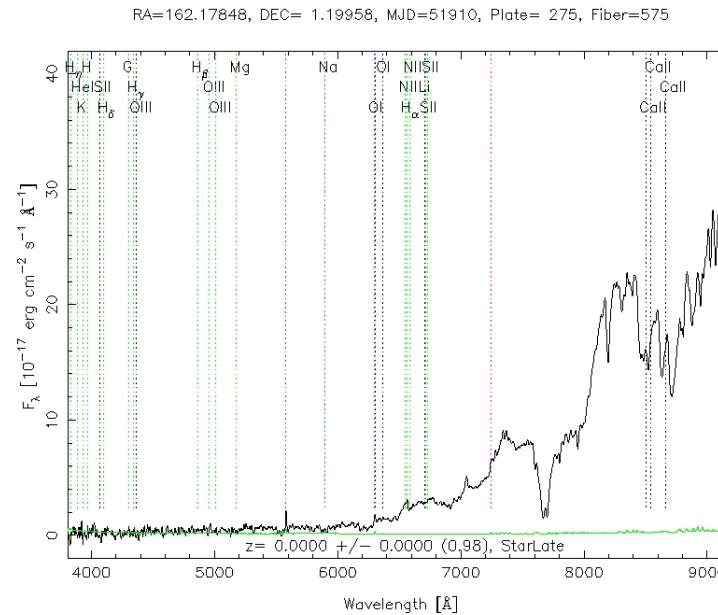
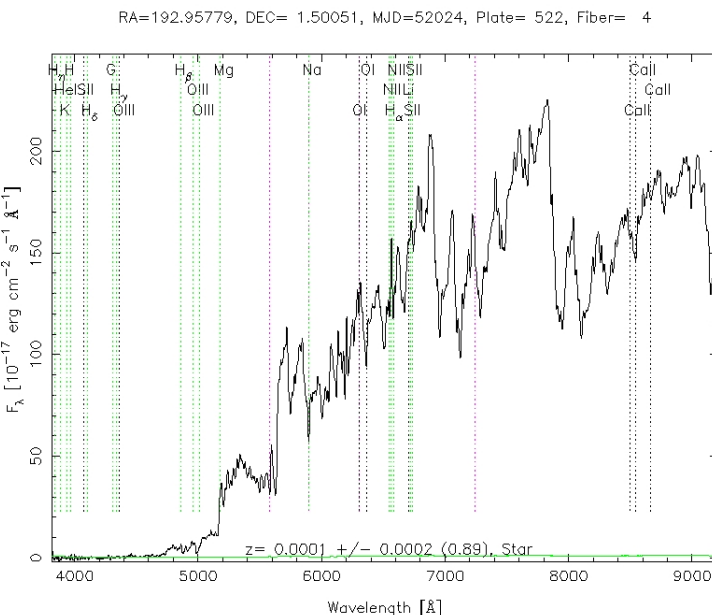
1. More accurate and robust **source identification** than based on photometric data alone: e.g. confirmation of unresolved binaries, low-metallicity stars, cold white dwarfs, L and T dwarfs, C stars, CVs, etc.
2. Accurate **stellar parameters estimation** ( $T_{\text{eff}}$ ,  $\log(g)$ , metallicity, detailed chemical composition)
3. **Radial velocity** for kinematic studies of the Milky Way (especially useful when combined with proper motions)
4. **Calibration** of observations (e.g. can synthesize photometry with an accuracy of  $\sim 0.04$  mag)

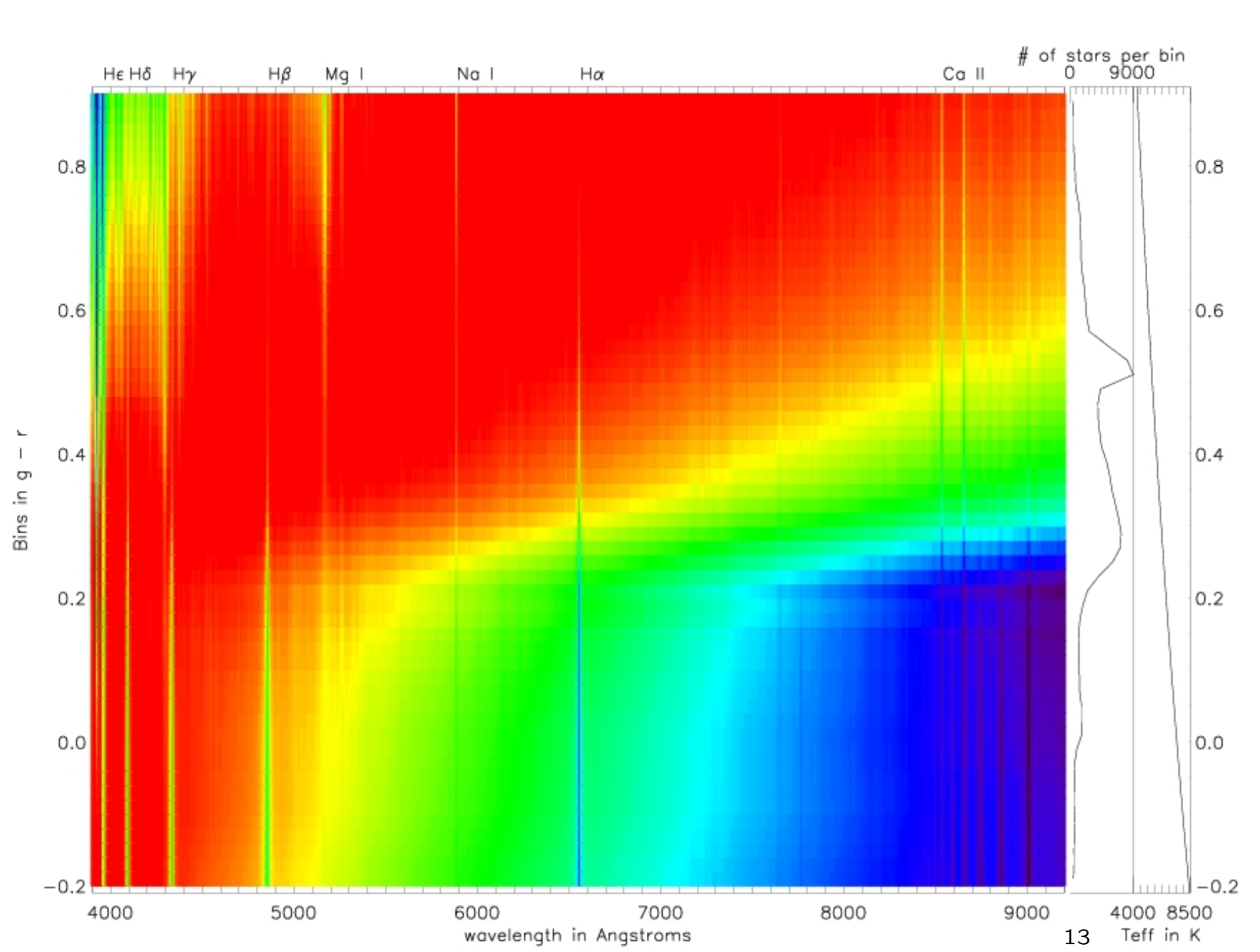


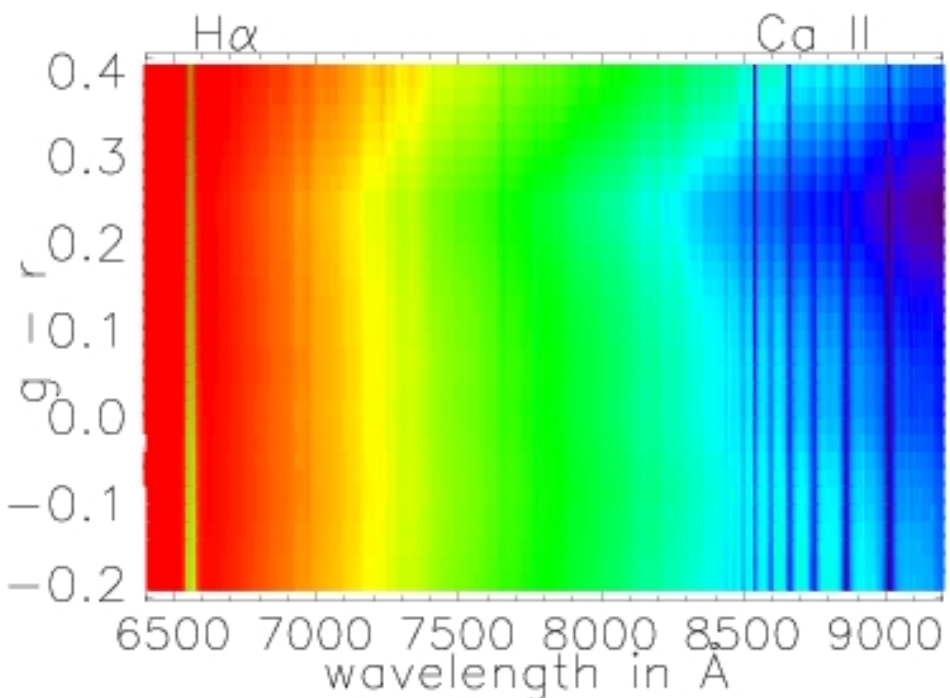
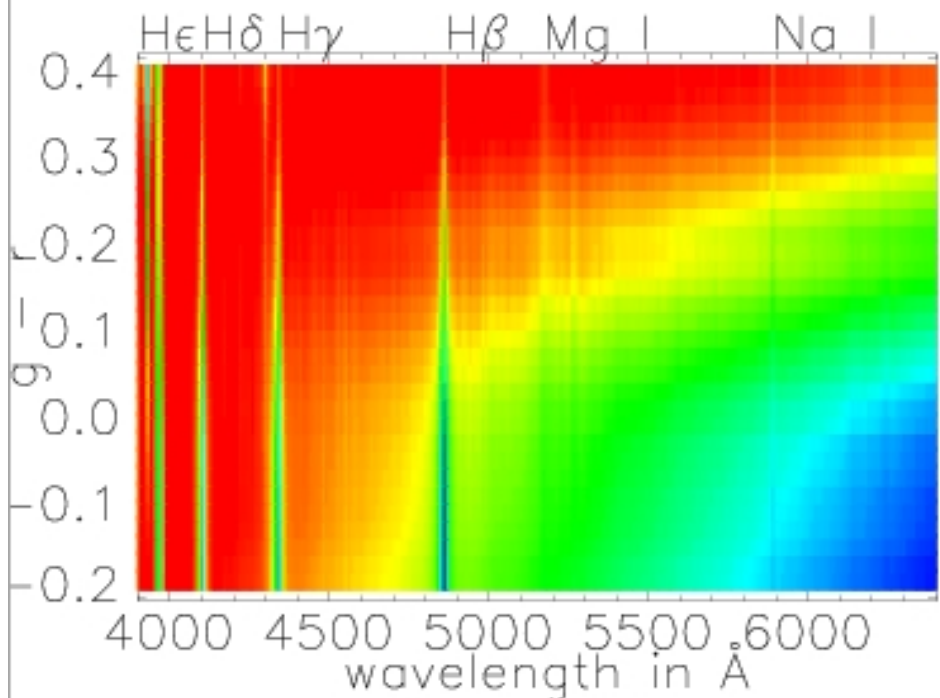
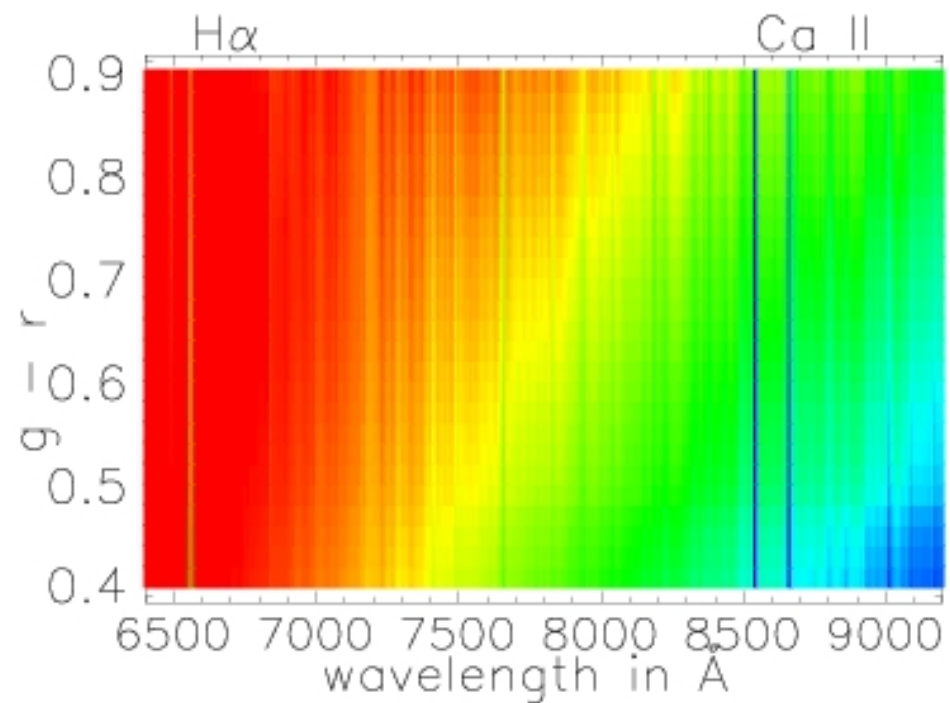
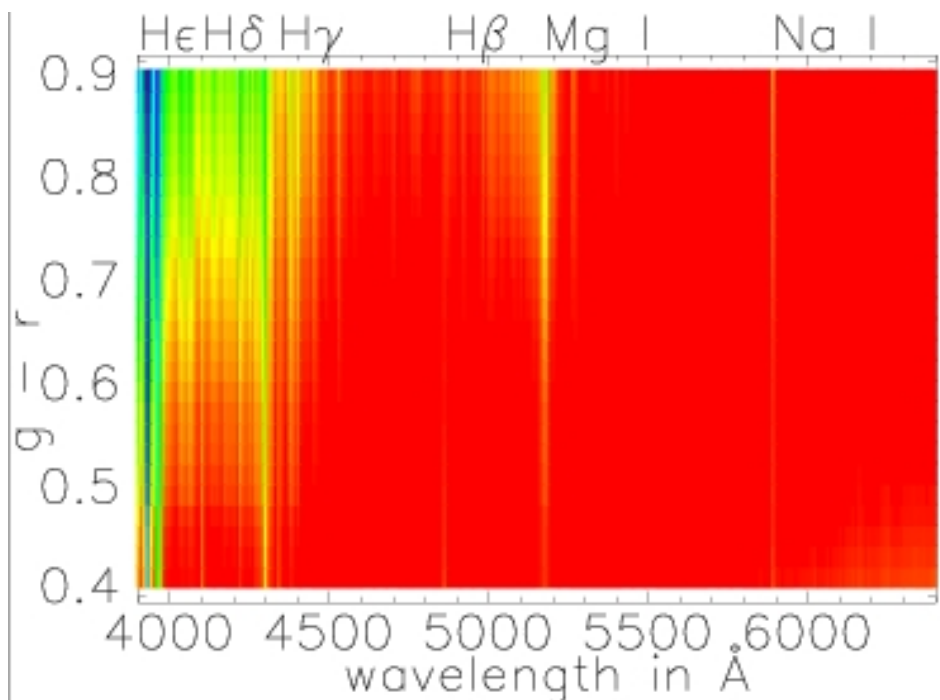


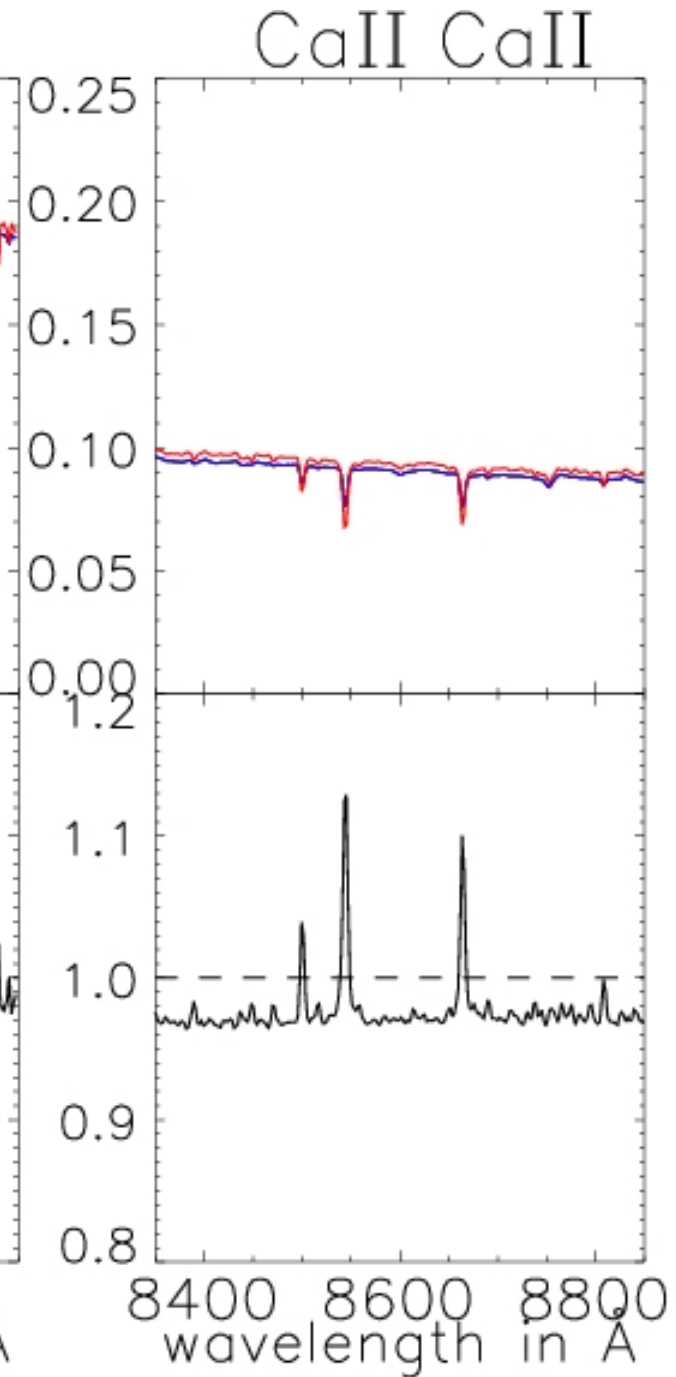
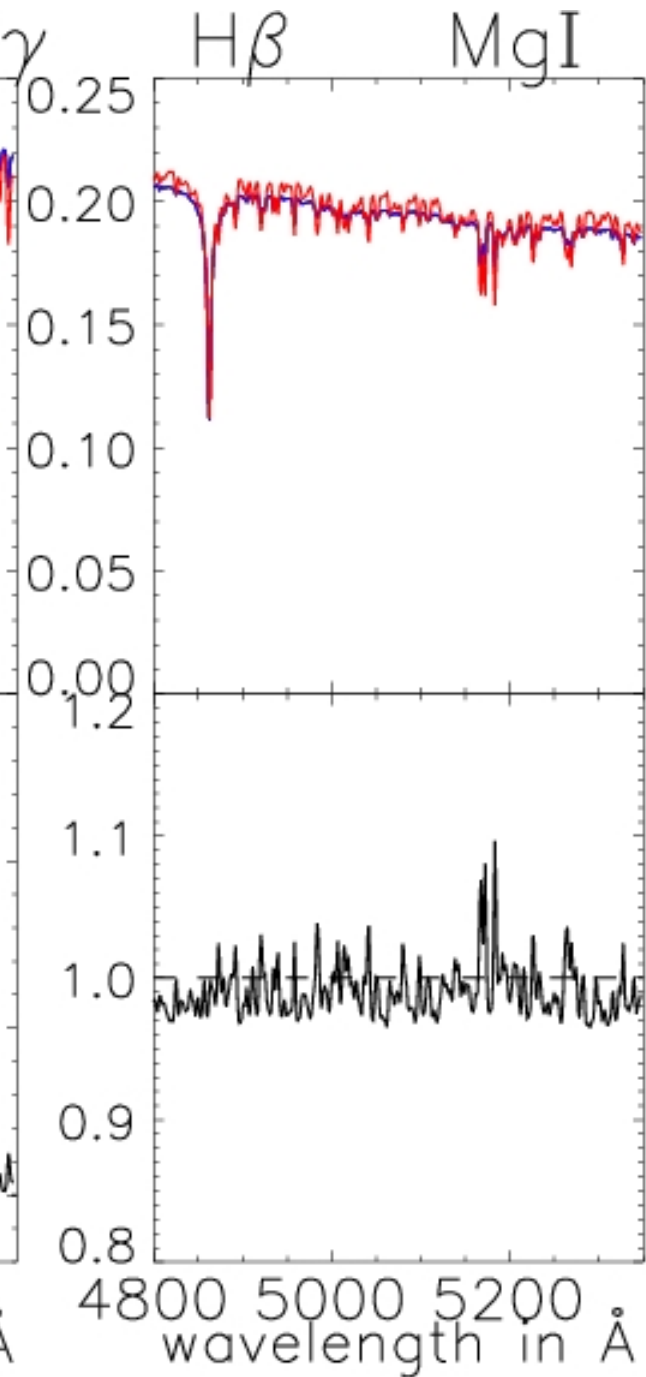
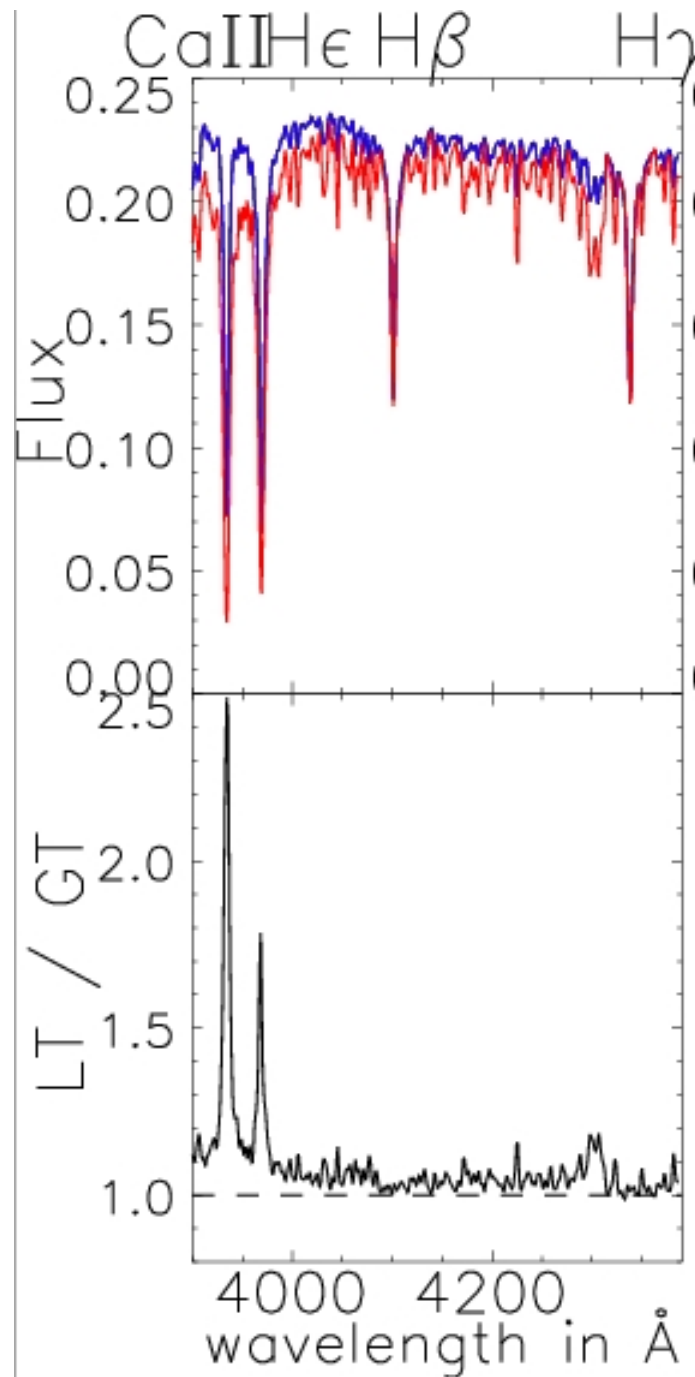
## Source Identification

- Stellar spectroscopic targets are color-selected, as illustrated in the **top left** figure
- A spectrum is required to secure a robust identification, as well as for a detailed measurement of the source properties
- **Bottom left:** an example of a C star: SDSS has discovered 95% of all known dwarf C stars (Margon et al. 2006)
- **Bottom right:** an example of an L dwarf (SDSS has discovered the first known field T dwarf, Strauss et al. 2000)



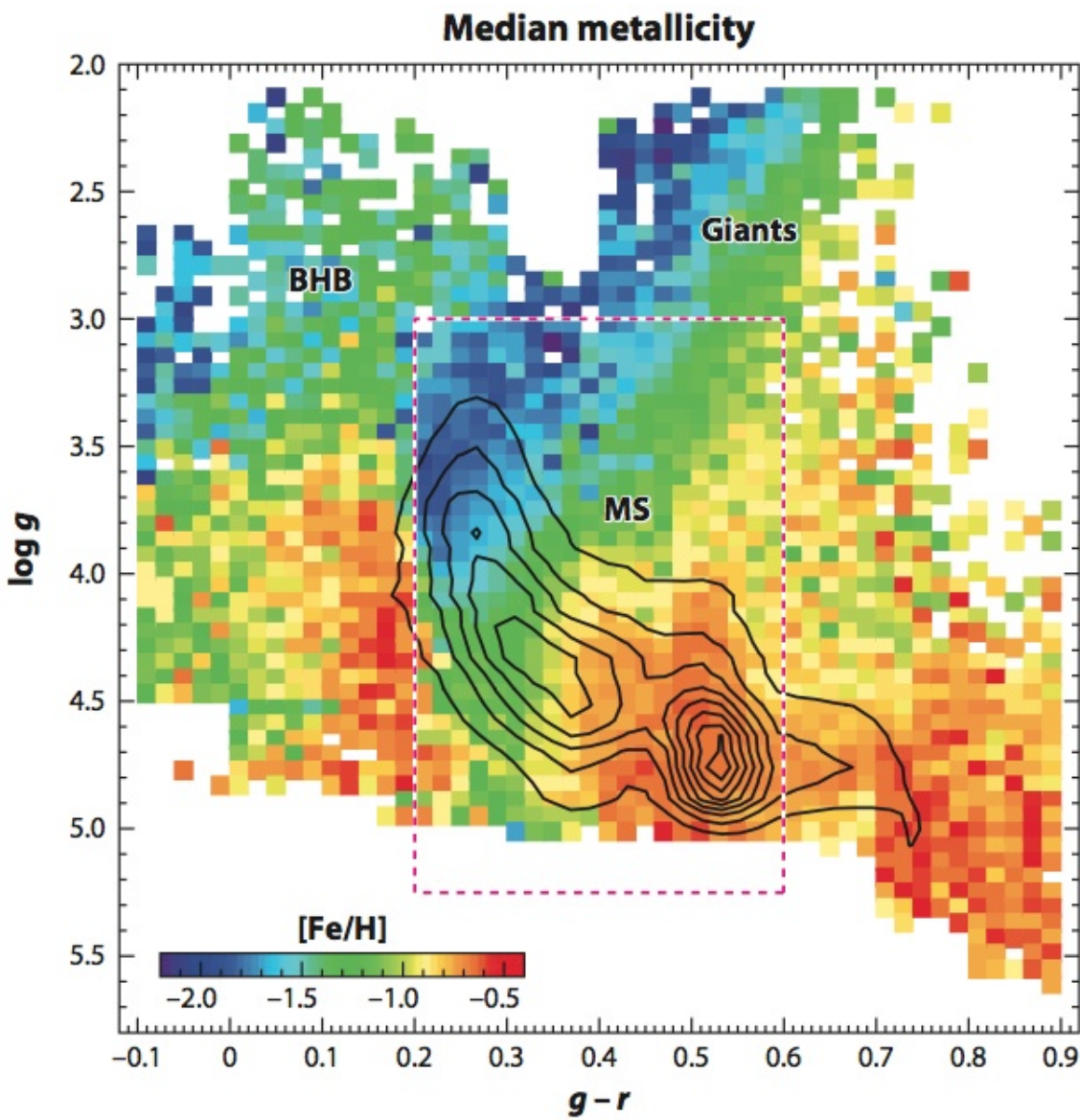


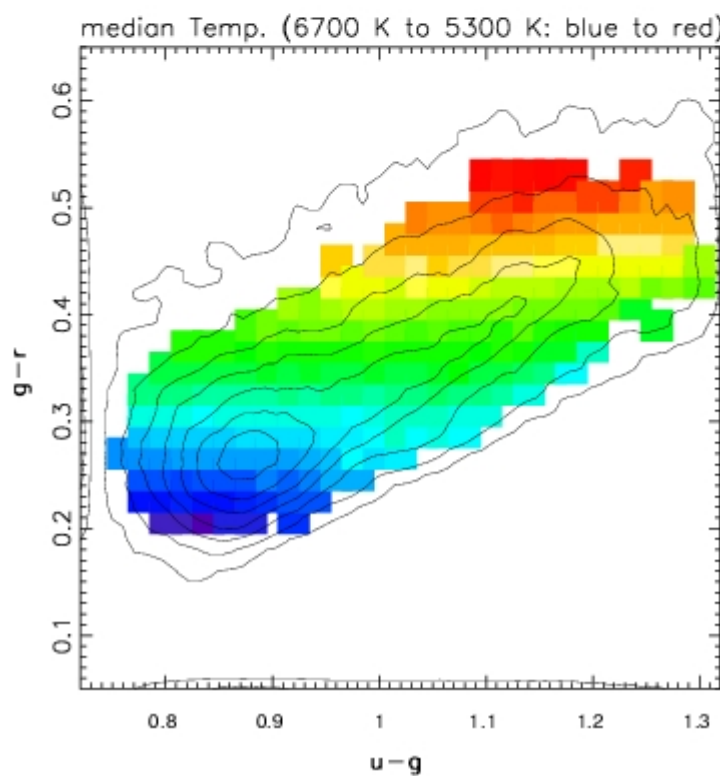
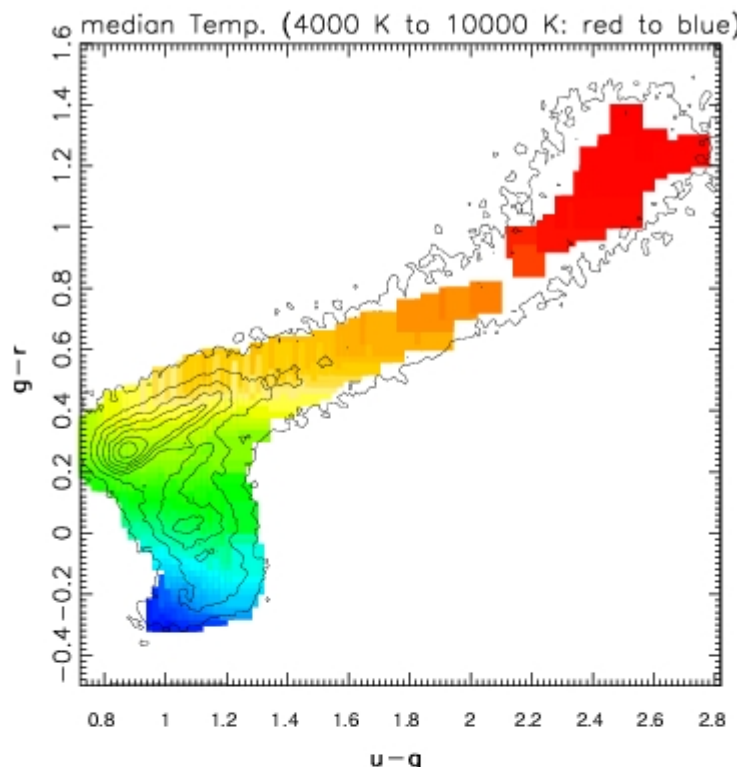




## Stellar Parameters Estimation

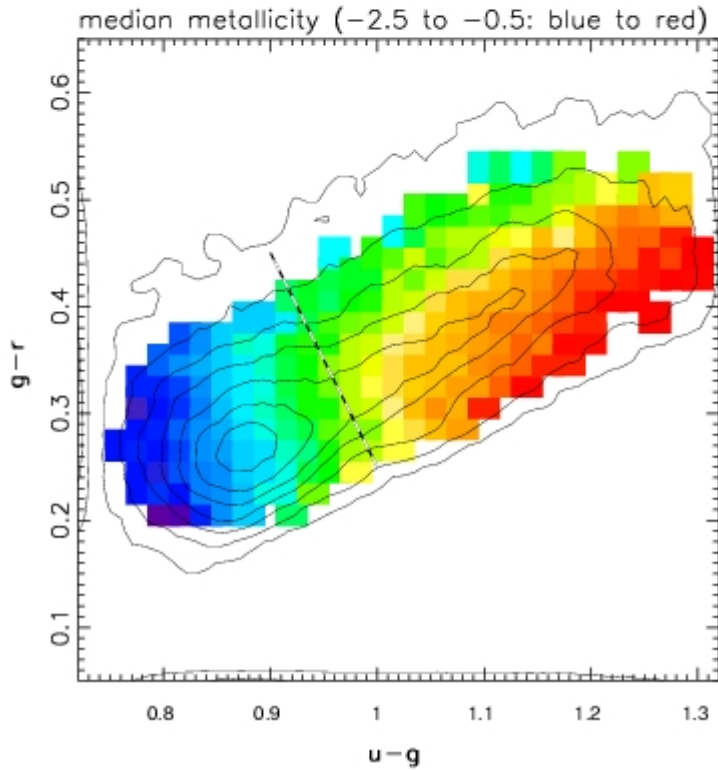
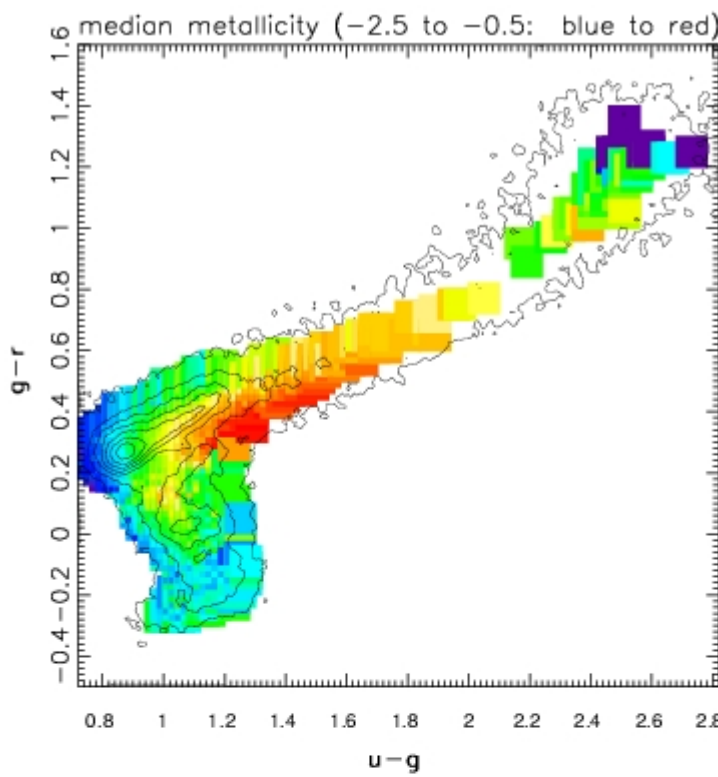
- SDSS stellar spectra are automatically processed to obtain stellar parameters such as **effective temperature, gravity, metallicity**.
- **Left:** resembles a warped HR diagram; the color-coded map shows the median metallicity as a function of  $\log(g)$  (roughly, dwarfs vs. giants) and the  $g-r$  color (roughly, effective temperature), according to the legend in the bottom left corner; the contours show the distribution of all SDSS stars with spectra (biased!)





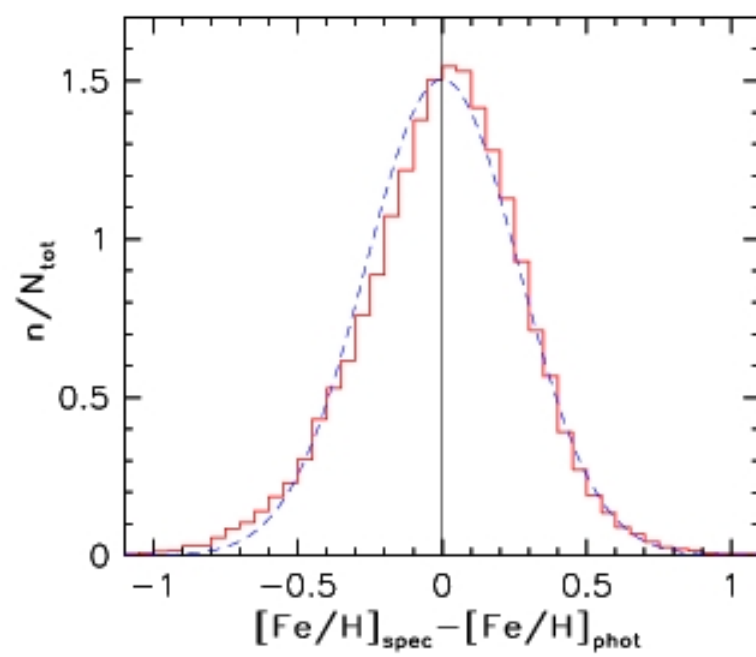
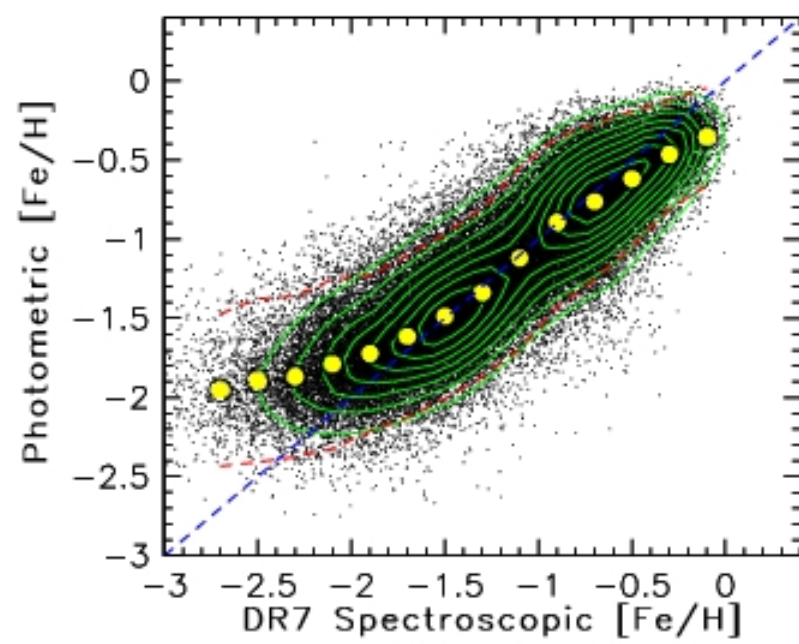
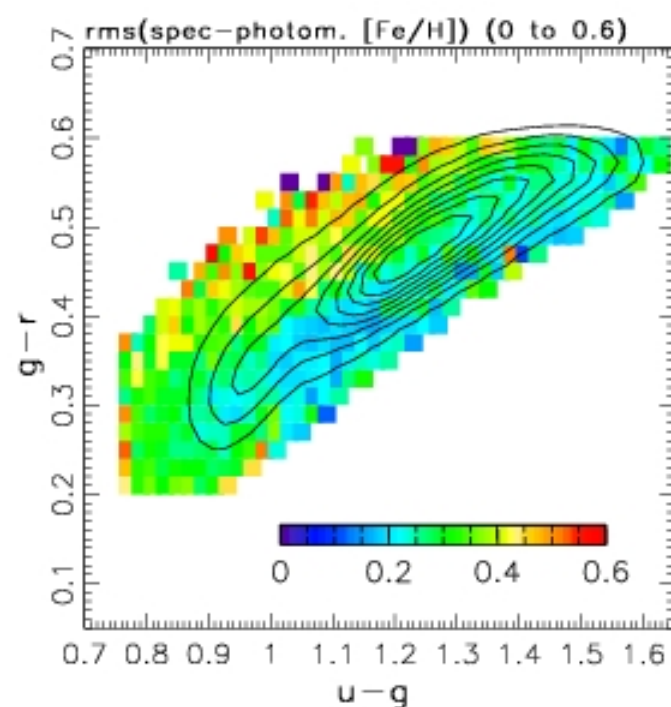
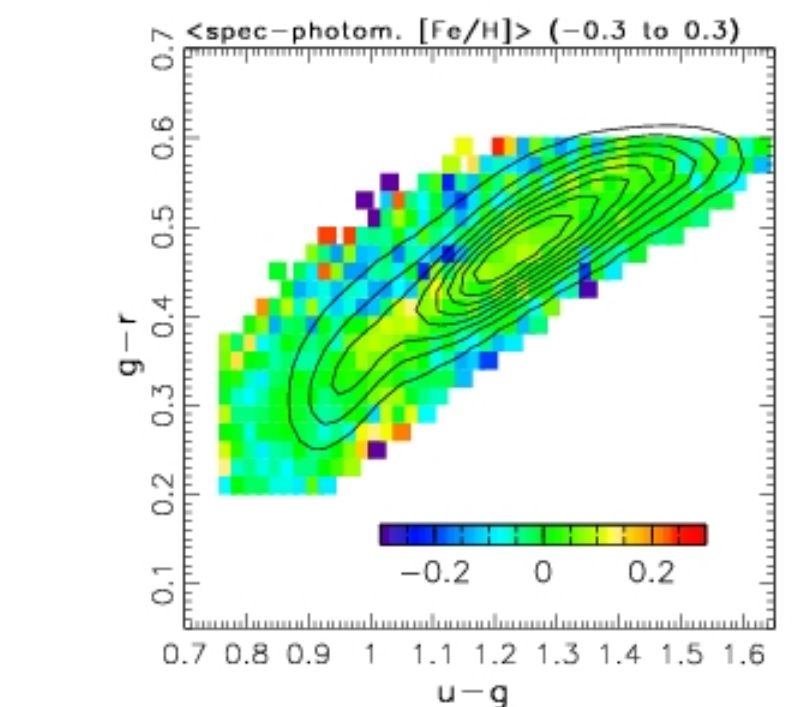
## Stellar Parameters Estimation: $T_{eff}$

- SDSS stellar spectra are of sufficient quality to provide robust and accurate stellar parameters such as **effective temperature, gravity, metallicity**, and detailed chemical composition
- Stellar parameters estimated from spectra show a good correlation with colors measured from imaging data
- Top left:** the median effective temperature as a function of the position in the  $g - r$  vs.  $u - g$  diagram (from 4000 K to 10,000 K, red to blue)
- Bottom left:** zoomed-in version of the top left figure
- Photometric estimate of effective temperature:**  $T_{eff}$  determines the  $g - r$  color, but has negligible impact on the  $u - g$  color



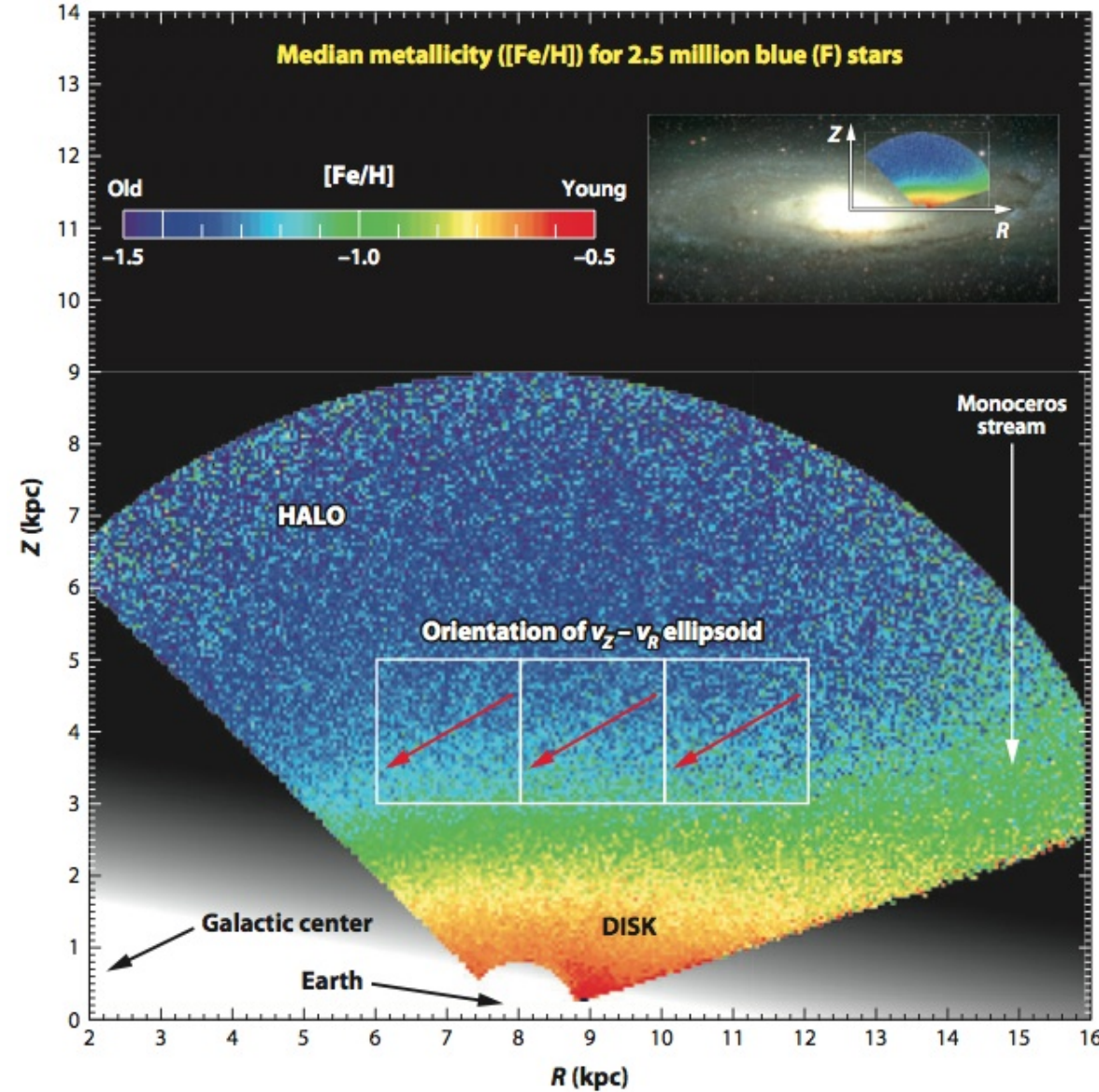
## Stellar Parameters Estimation: [Fe/H]

- Stellar parameters estimated from spectra show a good correlation with colors measured from imaging data
- **Top left:** the median metallicity as a function of the position in the  $g - r$  vs.  $u - g$  diagram ( $-0.5$  to  $-2.5$ , red to blue)
- **Bottom left:** zoomed-in version of the top left figure
- **Photometric estimate of metallicity:** can be determined with an error of  $\sim 0.2\text{-}0.3$  dex (relative to spectroscopic estimate) from the position in the  $g - r$  vs.  $u - g$  color-color diagram using simple expressions
- This finding is important for studies based on photometric data alone, and also demonstrates the robustness of parameters estimated from spectroscopic data



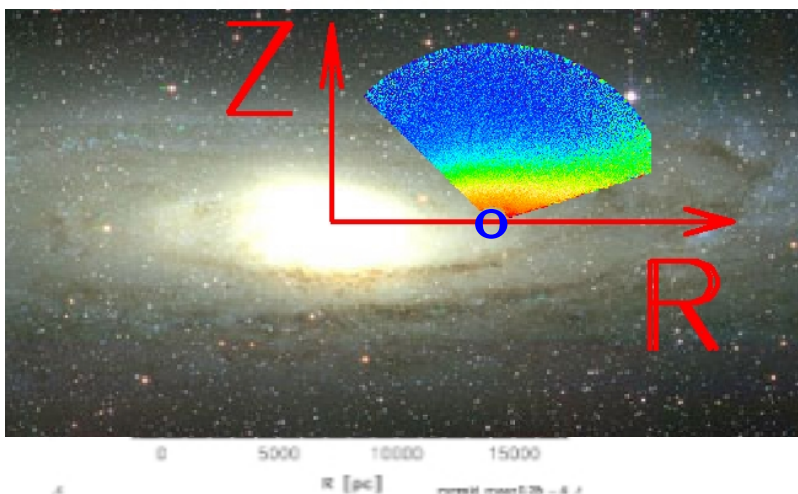
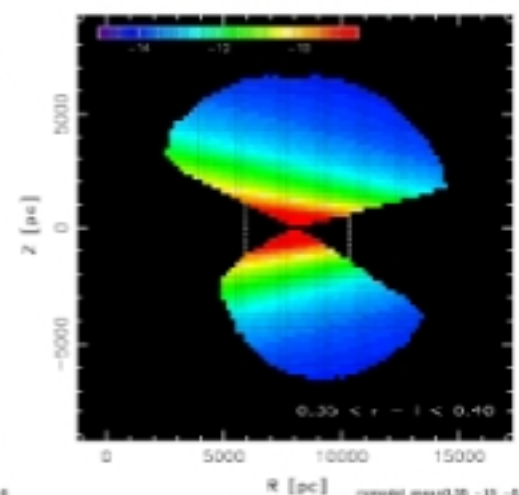
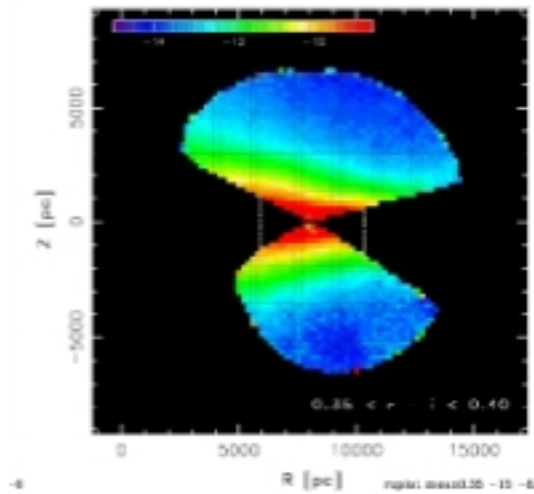
## Photometric Metallicity Distribution

- Panoramic view of the Milky Way metallicity distribution: the median metallicity map contains  $\sim 8,000$  pixels ( $0.1$  kpc by  $0.1$  kpc), and is based on a complete flux- and color-limited sample of  $\sim 2.5$  million blue stars.
- The median metallicity is a strong function of distance from the Galactic plane; deviations are associated with spatial (and kinematic) substructures



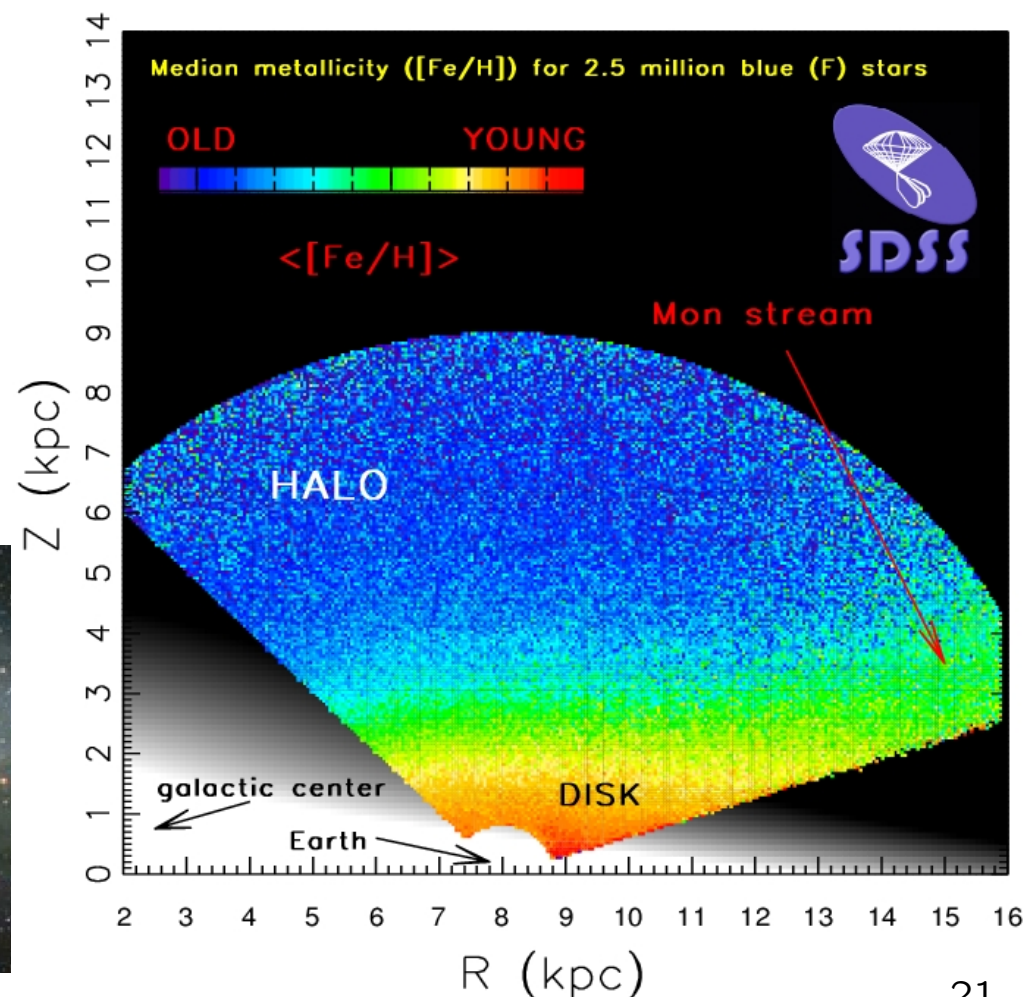
A much harder analysis problem than counts; instead of a single count value, at each position:  
 $p([{\rm Fe}/{\rm H}])$  and  $p(v_\phi, v_R, v_Z)$  !

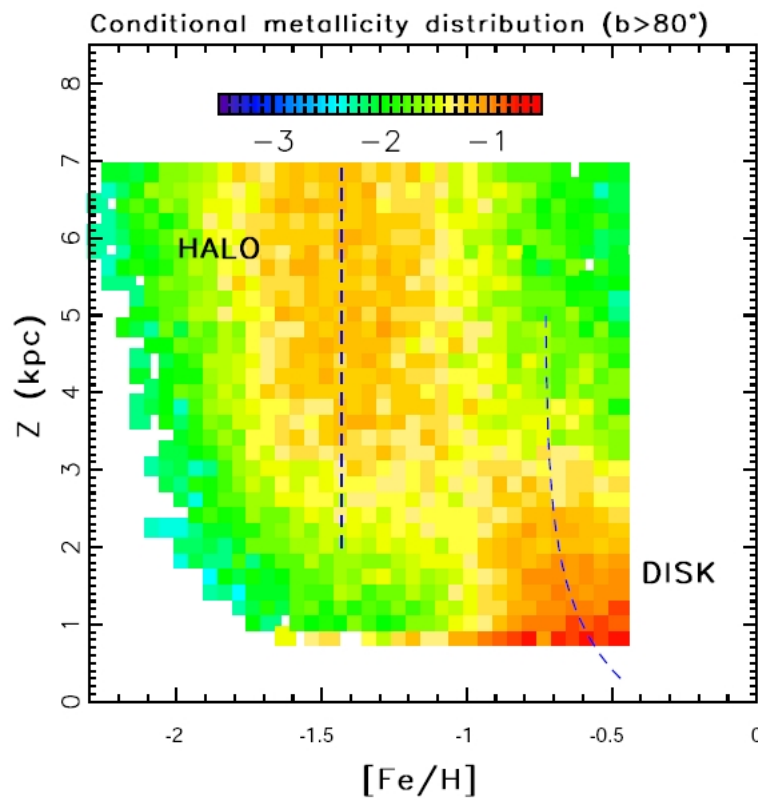
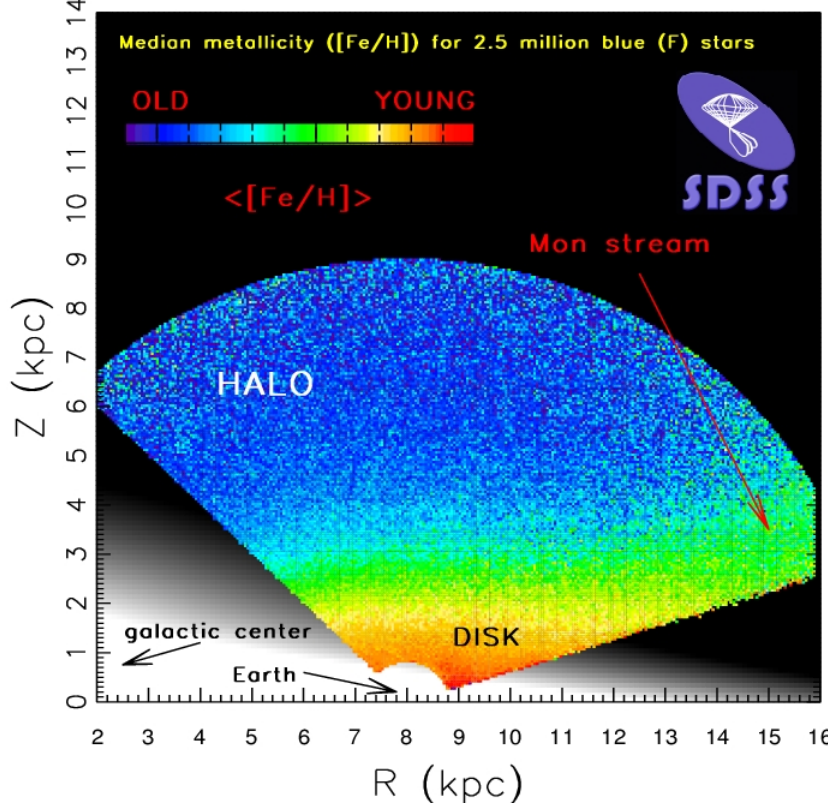
$0.35 < r-i < 0.40$



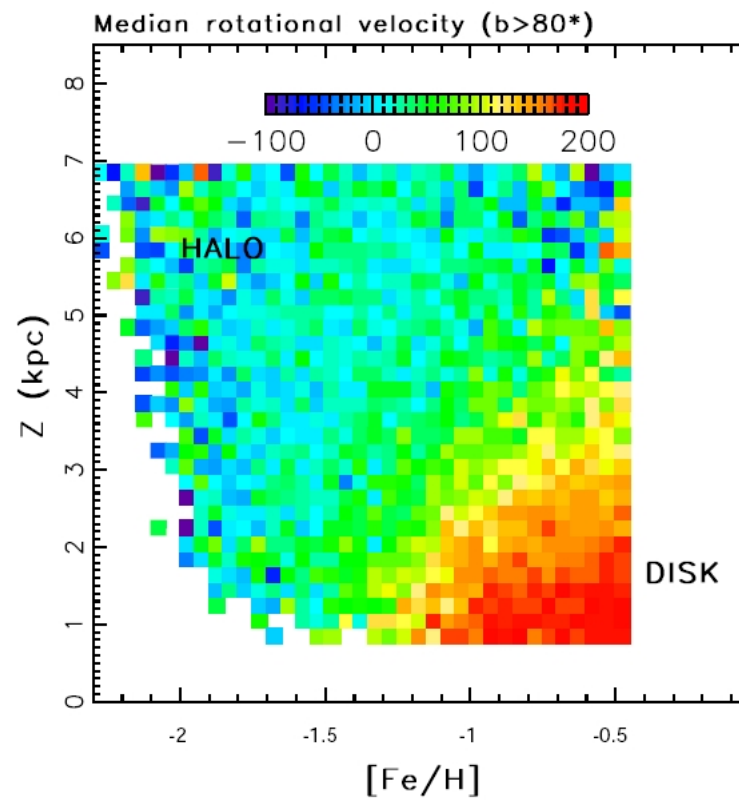
## Dissecting the Milky Way with SDSS

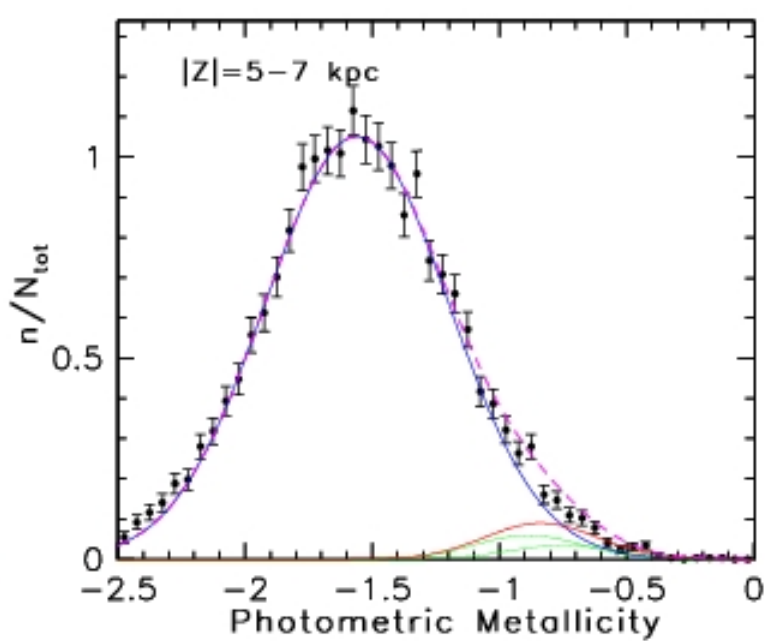
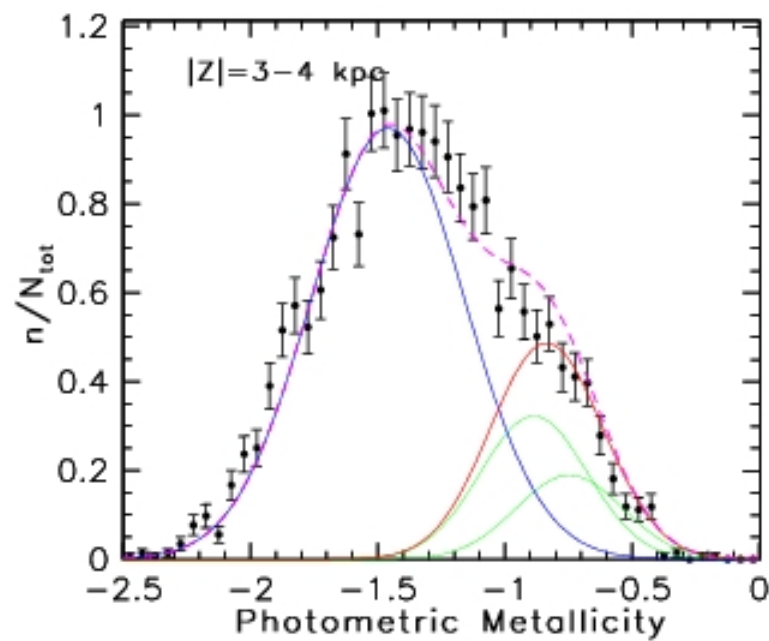
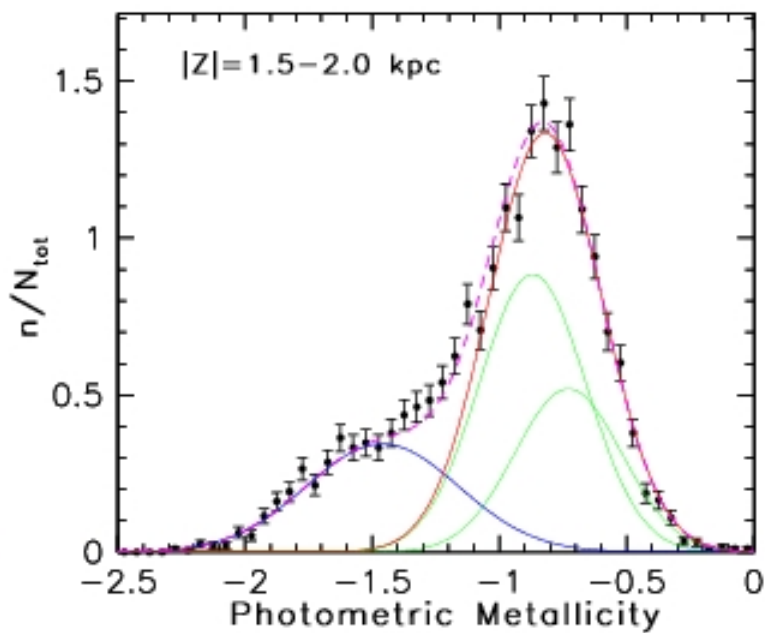
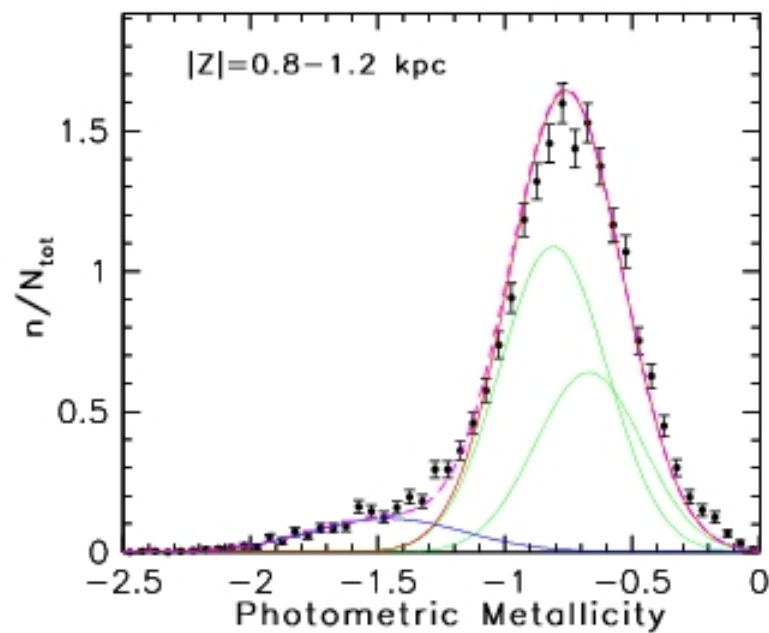
- Panoramic view of the Milky Way, akin to observations of external galaxies; good support for standard Galactic models (with amazing signal-to-noise!)
- Metallicity mapping supports components inferred from number counts mapping

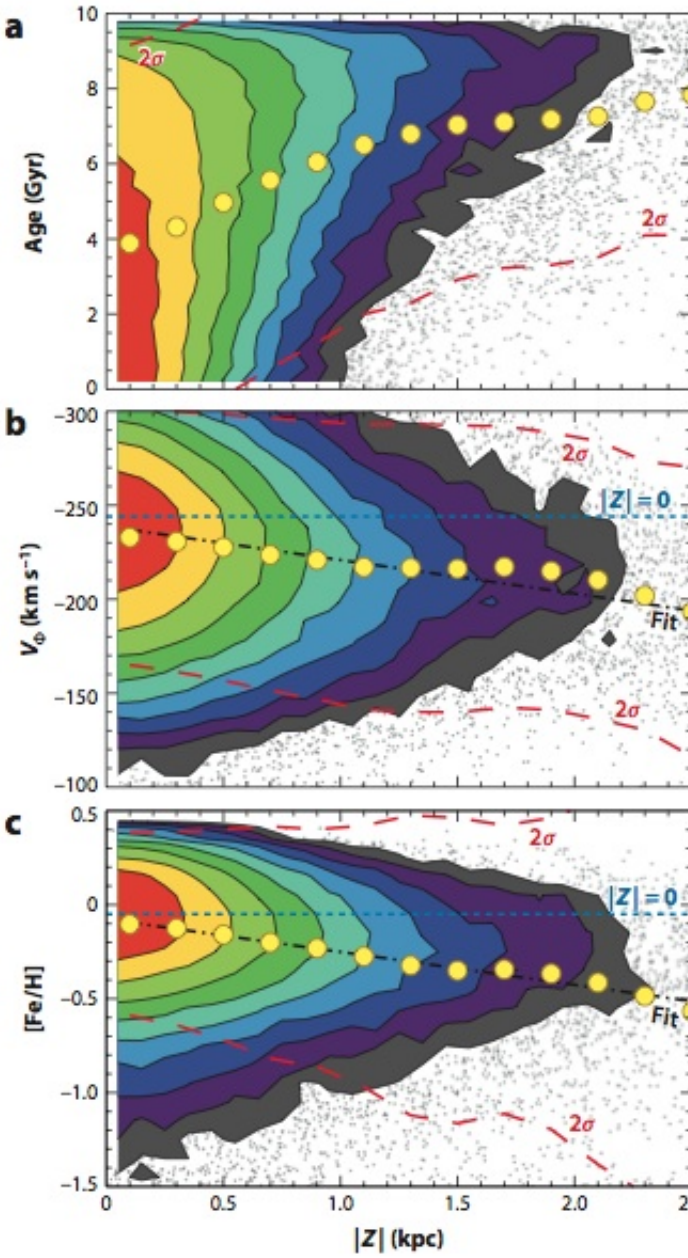




- ## Metallicity and Kinematics
- Metallicity mapping supports components inferred from number counts mapping: remarkable disk–halo separation!
  - Kinematics correlated with metallicity: high-metallicity (disk) stars rotate, low-metallicity (halo) stars on random highly eccentric orbits

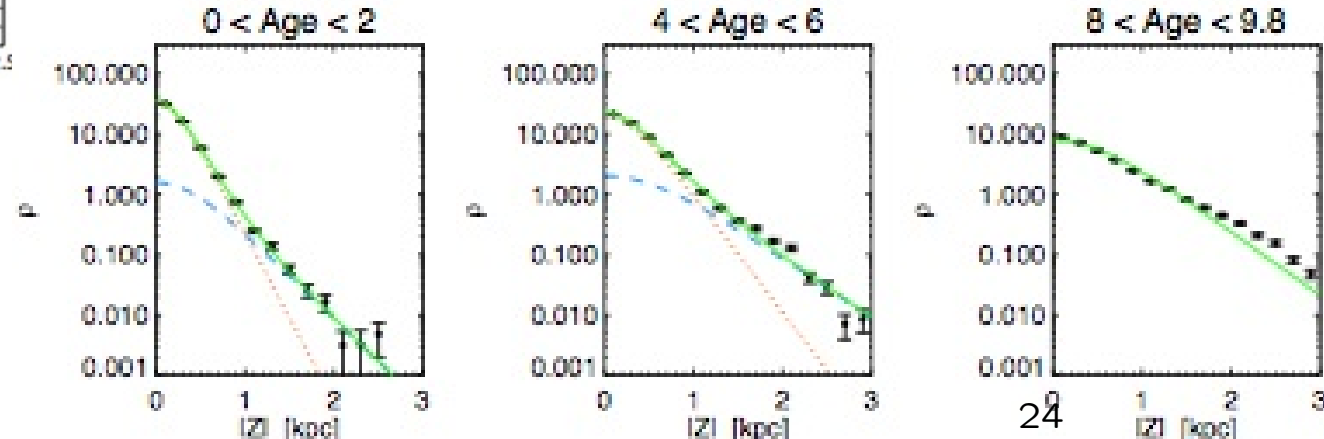


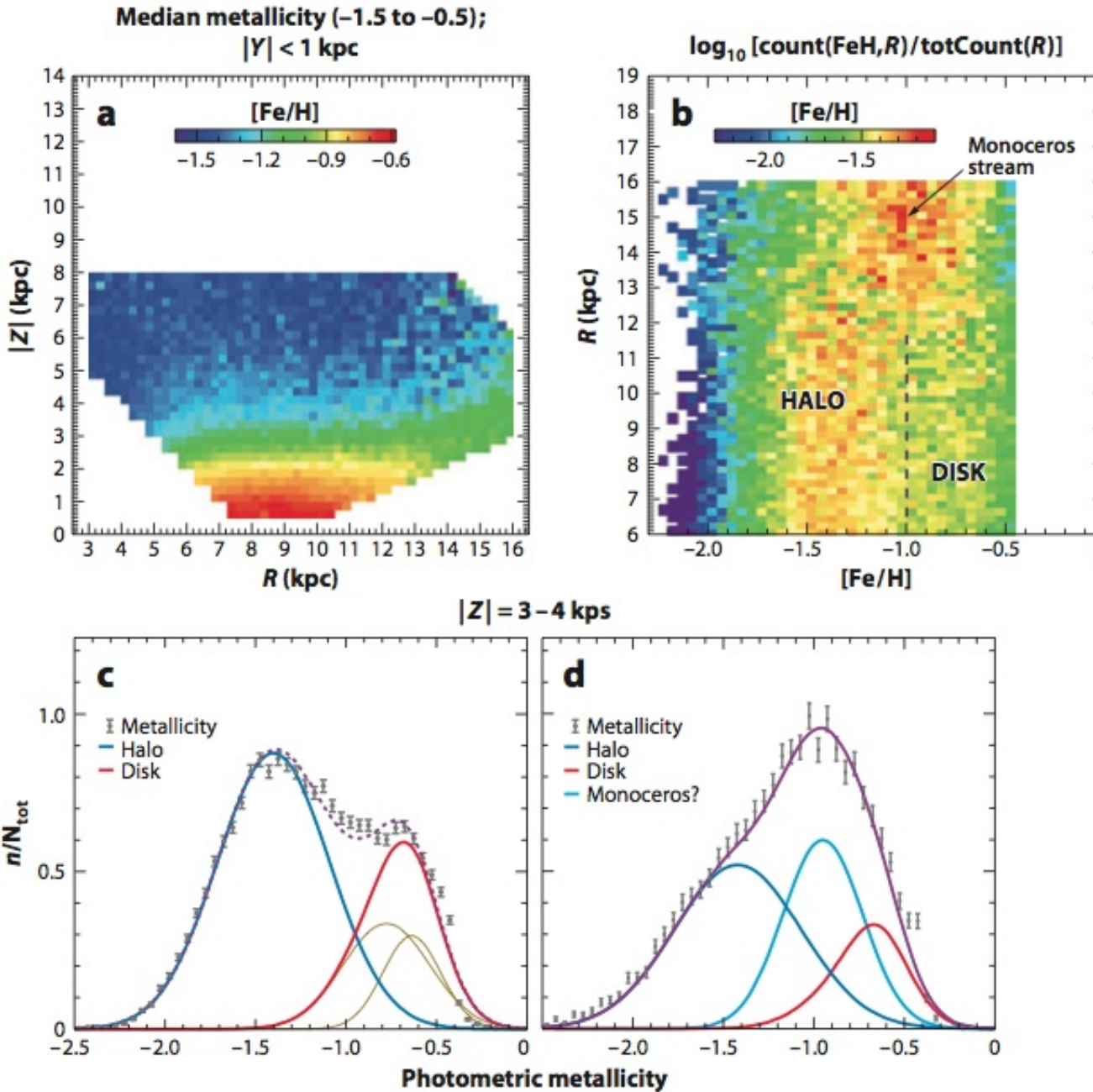




**Loebman et al. 2011**  
**(ApJ, 737, 17)**  
**(Roškar et al. models)**

- ## Thin/Thick Disk is an Age Effect!
- **Data:** Change of slope of stellar counts at  $\sim 1$  kpc, and both rotational velocity distribution and metallicity distribution for disk stars vary with  $Z$
  - N-body models with radial migration:
    - 1) behave like the data, and
    - 2) provide age information and details about radial migration
  - **Models:** Older stars
    - 1) reach larger  $|Z|$ ,
    - 2) have lower  $[Fe/H]$ ,
    - 3) display rotational velocity lag,
    - 4) no  $[Fe/H]-v_\phi$  correlation**Observers call this behavior “thick disk”**





## Metallicity Substructure

- Monoceros stream was discovered using stellar counts
- It is also identified as a substructure in metallicity space... LEFT
- And kinematics, too: it rotates faster than LSR by  $\sim 50 \text{ km/s}$
- More details: Ivezić et al. 2008 (ApJ 684, 287)

**There is fine substructure in the metallicity distribution!**

## [ $\alpha$ /Fe] distribution for disk stars

- 17,000 G dwarfs with SDSS [ $\alpha$ /Fe] measurements (Lee et al. 2011).
- Bimodal distribution!
- Strongly suggests a thin/thick disk separation based solely on [ $\alpha$ /Fe] (age proxy?)

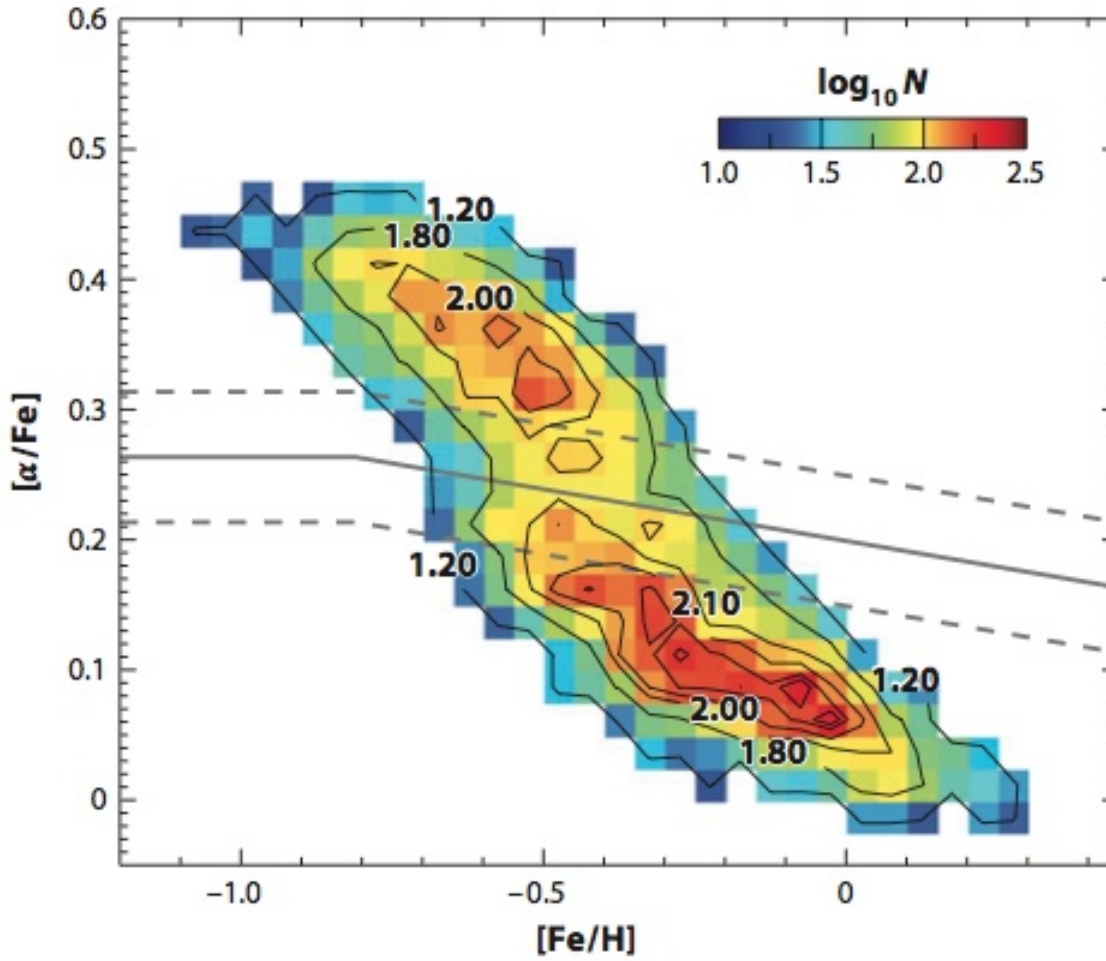
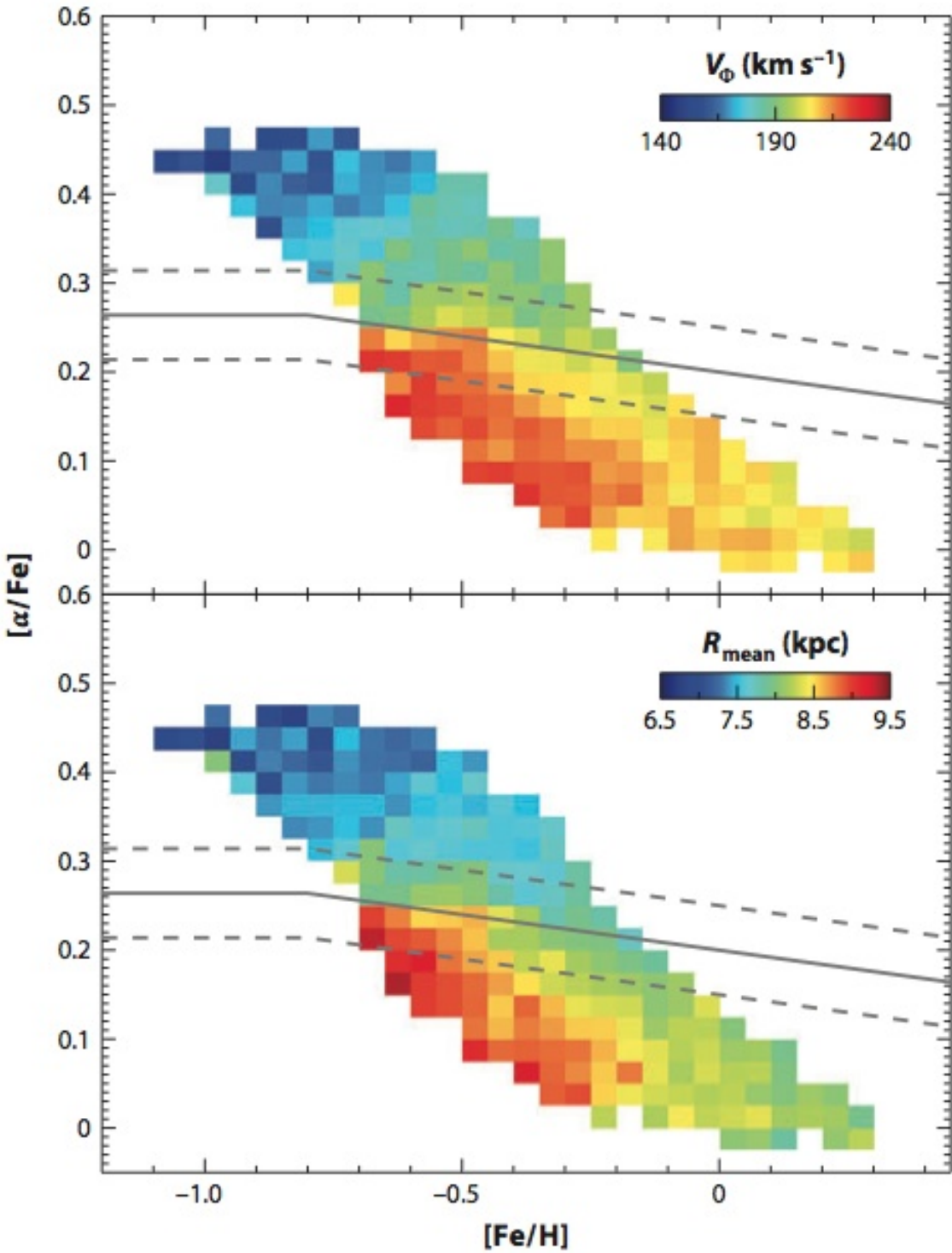


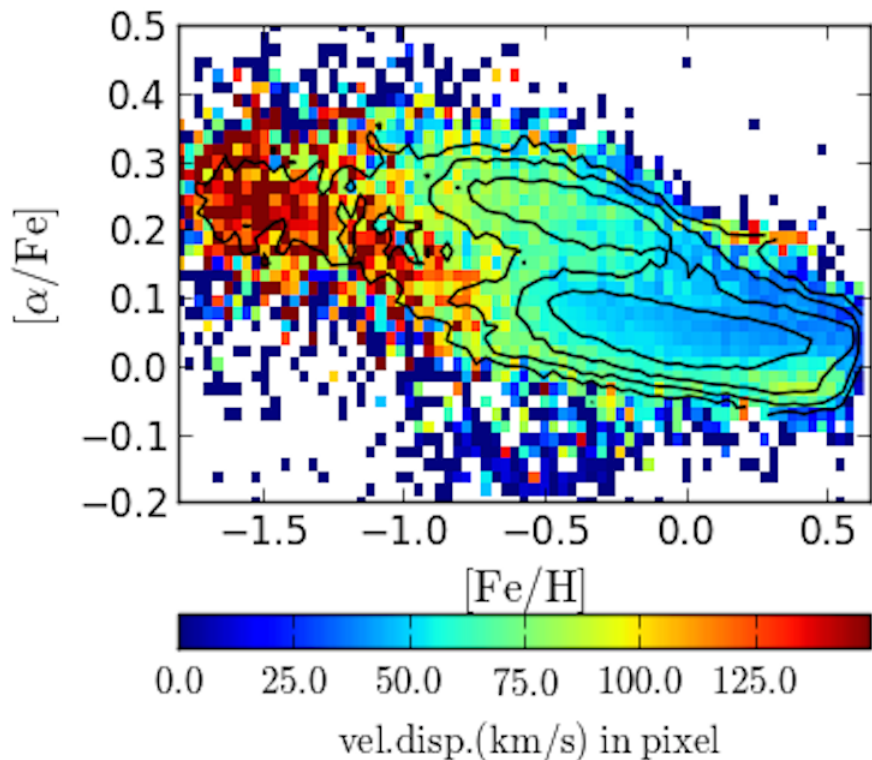
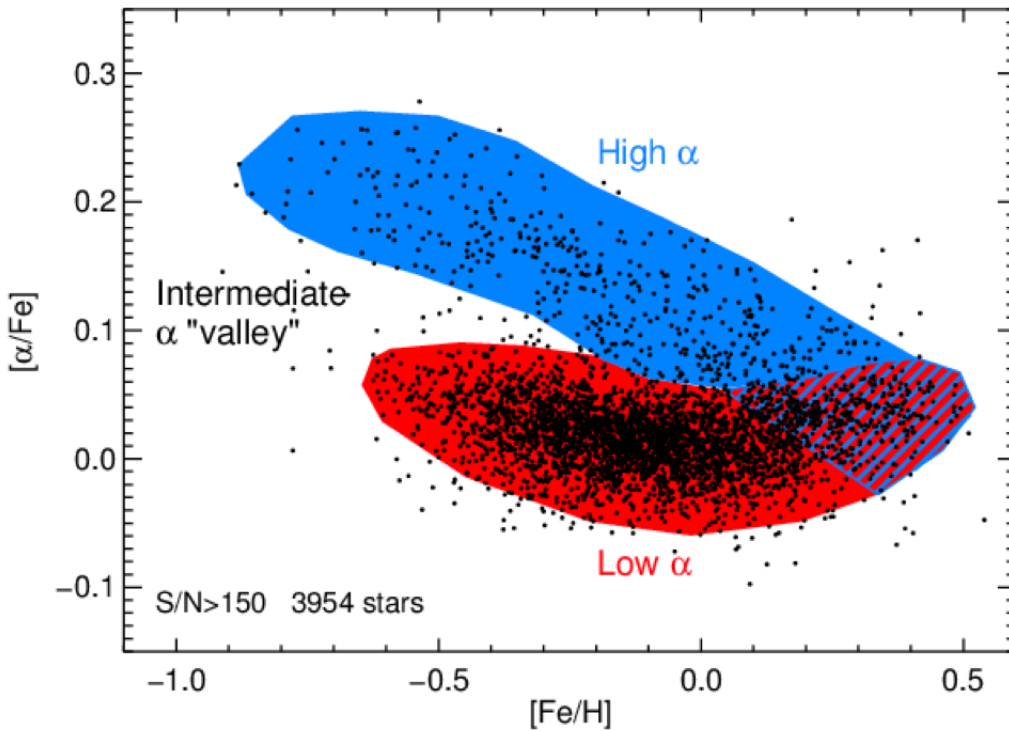
**Figure 8**

The [ $\alpha$ /Fe] versus [Fe/H] distribution of G-type dwarfs within a few kiloparsecs from the Sun. The number density (arbitrarily normalized) is shown on a logarithmic scale according to the legend and by isodensity contours. Each pixel (0.025 dex in the [ $\alpha$ /Fe] direction and 0.05 dex in the [Fe/H] direction) contains at least 20 stars (with a median occupancy of 70 stars). The distribution of disk stars in this diagram can be described by two components (thin disk and thick disk, respectively) centered on ( $[Fe/H]$ ,  $[\alpha/Fe]$ ) =  $(-0.2, +0.10)$  and  $(-0.6, +0.35)$ . The solid gray line is the fiducial for division into likely thin- and thick-disk populations; note that a simple  $[\alpha/Fe] = 0.24$  separation results in almost identical subsamples. The dashed gray lines show the selection boundaries adopted by Lee et al. (2011b), which exclude the central overlap region. Adapted from Lee et al. (2011b).



## $[\alpha/Fe]$ distribution for disk stars

- Strong correlation of orbital parameters (top: rotational velocity; bottom: mean orbital radius) with the position in the  $[\alpha/Fe]$  vs.  $[Fe/H]$  plane.
- Bovy, Rix & Hogg (2012) claim a continuous behavior rather than a two-component decomposition.
- The differences in  $[\alpha/Fe]$  likely reflect different star-formation timescales (enrichment by Type Ia versus Type II supernovae for low and high  $[\alpha/Fe]$  values over long and short timescales, respectively), see Bensby et al. (2004).



## [ $\alpha/\text{Fe}$ ] distribution for disk stars

- Latest news from Nidever, Bovy et al. (2014, ApJ 796, 38): “The clear  $[\alpha/\text{Fe}]$  bimodality in the APOGEE data . . . and we confirm this result . . . and find that it is not caused by selection effects.”
- With APOGEE measurements (SDSS Data Release 12, bottom left), the observed bimodality is self-evident. Also, note contamination by halo stars at  $[\text{Fe}/\text{H}] < -1$ , easily recognized from elevated velocity dispersion.